

Screenshot of the ScholarOne Manuscripts Author Dashboard. The page title is "Numerical Methods for Partial Differential Equations". The dashboard shows a sidebar with navigation options: Home, Author, Review. The main content area is titled "Manuscripts with Decisions" and contains a table with the following data:

ACTION	STATUS	ID	TITLE	SUBMITTED	DECISIONED
a revision has been submitted (NMPDE-2020-3405.R1)	EIC: Webster, Clayton ADM: Editorial, Office	NMPDE-2020-3405	A Modified Walk-on-sphere Method for High Dimensional Poisson Equation <a href="#">View Submission</a>	28-Jul-2020	22-Dec-2020

Additional information in the table row:

- Major Revision (22-Dec-2020)
- a revision has been submitted

Links below the table: [view decision letter](#), [Contact Journal](#)

# A Modified Walk-on-sphere Method for High Dimensional Fractional Poisson Equation<sup>1</sup>

Caiyu Jiao<sup>a</sup>, Changpin Li<sup>a,\*</sup>, Hexiang Wang<sup>b</sup>, Zhongqiang Zhang<sup>c</sup>

<sup>a</sup>*Department of Mathematics, Shanghai University, Shanghai 200444, China*

<sup>b</sup>*School of Mathematics and Statistics, Kashi University, Kashi 844006, Xinjiang, China*

<sup>c</sup>*Department of Mathematical Sciences, Worcester Polytechnic Institute, Worcester, MA 01609 USA*

## Abstract

We develop walk-on-sphere method for fractional Poisson equations with Dirichlet boundary conditions in high dimensions. The walk-on-sphere method is based on probabilistic representation of the fractional Poisson equation. We propose efficient quadrature rules to evaluate integral representation in the ball and apply rejection sampling method to drawing

<sup>1</sup>Li and Wang were supported by the National Natural Science Foundation of China under grant nos. 11926319 and 11926336. Zhang was partially supported by ARO/MURI grant W911NF-15-1-0562.

from the computed probabilities in general domains. Moreover, we provide an estimate of the number of walks in the mean value for the method when the domain is a ball. We show that the number of walks is increasing in the fractional order and the distance of the starting point to the origin. We also give the relationship between the Green function of fractional Laplace equation and that of the classical Laplace equation. Numerical results for problems in 2-10 dimensions verify our theory and the efficiency of the modified walk-on-sphere method.

*Keywords:* walk on spheres, fractional Laplacian, modified walk-on-sphere method, inexact sampling

---

## 1. Introduction

The fractional Laplacian,  $(-\Delta)^s$ , is a prototypical operator for modeling nonlocal and anomalous phenomenon which incorporates long range interactions [30]. It arises in many areas of applications, including models for turbulent flows, porous media flows, pollutant transport, quantum mechanics, stochastic dynamics, and finance [11, 20, 21, 34].

Numerical methods for fractional Laplacian operator and differential equations with fractional Laplacian operator have been investigated in dozens of papers, such as in finite difference methods [15, 22, 28], spectral methods [2, 38, 19], finite element methods [1, 4, 14] and probabilistic methods [18, 26]. See review papers [6, 31, 13] for more details. All these methods are nonlocal and thus expensive in high dimensions, except the probabilistic methods. While the most economical method is with quasi-linear complexity in number of physical nodes [4] using finite element methods in 2D, no numerical results are reported for Poisson equation with fractional Laplacian over general bounded domain in high dimensions such as in three or much higher dimensions.

Probabilistic methods (usually implemented with Monte Carlo methods, say, for example, [24, 27]) for partial differential equations with/without fractional Laplacian are based on the probabilistic representation of the Laplacian/fractional Laplacian, see e.g. [5]. These methods do not require any discretization in space. In one of such methods, walk-on-sphere method (e.g. [33]) does not even require discretization in time or even the diffusion trajectory of the stochastic process. Such probabilistic methods are particularly advantageous when the geometry domain  $\Omega$  is very complex or if the solution of the partial differential equation is required at a relatively small number of points.

Though Monte Carlo methods need  $\mathcal{O}(M^2)$  walks to achieve standard deviation  $\mathcal{O}(M^{-1})$ , it is a reliable method in arbitrarily high dimensions. In addition, they can be efficiently implemented on massively parallel computers.

In this work, we develop efficient probabilistic methods in high dimensions for the following fractional Poisson equation on an open bounded domain with an extended Dirichlet

---

\*Corresponding author. E-mail: lcp@shu.edu.cn

boundary value condition (see e.g. in [36]):

$$\begin{cases} (-\Delta)^s u(x) = f(x), & x \in \Omega, \\ u(x) = g(x), & x \in \mathbb{R}^n \setminus \Omega, \end{cases} \quad (1.1)$$

where  $s \in (0, 1)$ ,  $n \geq 1$  and we use the integral definition defined by a singular integral [35] which coincides with Riesz derivative definition on the whole space [8],

$$(-\Delta)^s u(x) = C(n, s) \text{P.V.} \int_{\mathbb{R}^n} \frac{u(x) - u(y)}{|x - y|^{n+2s}} dy. \quad (1.2)$$

Here P.V. stands for the Cauchy principle value and the constant  $C(n, s)$  is given by [8]

$$C(n, s) = \left( \int_{\mathbb{R}^n} \frac{1 - \cos \zeta_1}{|\zeta|^{n+2s}} d\zeta \right)^{-1} = \frac{s 2^{2s} \Gamma(\frac{n}{2} + s)}{\pi^{\frac{n}{2}} \Gamma(1 - s)} \quad (1.3)$$

with  $\zeta_1$  being the first component of  $\zeta = (\zeta_1, \zeta_2, \dots, \zeta_n) \in \mathbb{R}^n$  and  $\Gamma$  representing the Gamma function.

We develop our probabilistic method along the line of walk on spheres developed in [12, 17, 23, 26, 33, 37]. We use the modified walk-on-sphere method based on Poisson kernel and Green function to solve equation (1.1), which is also called ‘‘one point random estimation’’ (OPRE) method [12]. Specifically, every jump of one particle can be simulated with a certain probability until this particle is out of domain  $\Omega$  (see Figure 1) and all of the particles’ processes compose the approximate solution.

The difficulty in the implementation of this method is the computation of the probability in high dimensions, which hasn’t been addressed in literature. We will introduce some quadrature methods in Sections 2-4 and use rejection sampling method to draw samples whenever the exact sampling is not feasible. Another practical issue when implementing this approach is to estimate the average number of steps for it. When  $s \rightarrow 1$ , the Green function of fractional Laplacian equation is reduced to that of integer-order case. This issue is discussed in Section 4.

The contributions of this work are summarized as follows.

- We apply quadrature rules to the singular representation of walk on spheres and then numerically solve equation (1.1) in  $n$ -dimensional ball. We present some convergence analysis of the proposed approach. Compared with [26], we give the deterministic numerical method to solve equation in  $n$ -dimensional ball.
- We provide the modified walk-on-sphere method to numerically solve equation (1.1) on general domains in high dimensions. We find approximate probabilities of walk on spheres and draw samples from these probabilities. Compared with [26], the current work can be applied to arbitrary dimensions by rejection sampling method and reduces the computational time because of OPRE method. We illustrate the efficiency of the proposed approach using a numerical example of fractional Poisson equation in ten dimensions.

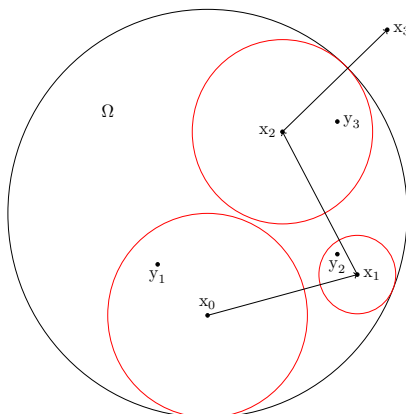


Figure 1: Steps of the modified walk-on-sphere algorithm until exiting the domain  $\Omega$

- We give an upper bound of the number of walks in the modified walk-on-sphere method for fractional Poisson equation in a ball. The upper bound is a function increasing with respect to the fractional order  $s$  and the distance of the starting point  $x_0$  to the origin. When  $s \rightarrow 1$ , Green function for the fractional Laplacian equation degenerates into that of the classical Laplace equation.

The rest of this paper is outlined as follows. In Section 2, we present the probabilistic representation for the homogeneous problem (1.1) where the domain  $\Omega$  is a ball. We also present quadrature rules to approximate the integrals in the representation.

In Section 3, we present the modified walk-on-sphere algorithm for the equation (1.1) on an open bounded domain  $\Omega$  in one dimension and high dimensions. For high dimensional problems, we present a simple and efficient rejection sampling method based on the truncated Gaussian distribution to draw samples from the probabilities of random walks.

In Section 4, we derive an estimate of number of walks for the method when the problem is considered on a ball. We show that the number of walks is increasing with respect to the fractional order and the distance of the starting point to the origin. We also give the relationship of Green functions between the fractional Laplacian and the classical Laplace equation.

In Section 5, numerical experiments are performed to confirm the convergent order of the proposed numerical evaluations in Section 2 and the efficiency of the modified walk-on-sphere method in Section 3. Finally, we summarize our work in the last section.

## 2. Probabilistic representation for fractional Poisson equation

In this section, we give an integral representation of  $u(x)$  in (1.1) where  $\Omega$  is a ball centered at  $x \in \mathbb{R}^n$ . The representation formula of the homogeneous equation is discretized by using quadrature formula and the corresponding error estimates are derived for  $n$  dimensional case.

### 2.1. Fractional Poisson equation on a ball

We start from equation (1.1) where  $\Omega$  is a ball centered at the origin with radius  $r > 0$ , i.e.,

$$\begin{cases} (-\Delta)^s u(x) = f(x), & x \in \mathbb{B}_r, \\ u(x) = g(x), & x \in \mathbb{R}^n \setminus \mathbb{B}_r. \end{cases} \quad (2.1)$$

To give the integral representation for  $u(x)$ , we introduce the following definitions.

**Definition 2.1.** ([7]) *Let  $r > 0$  be fixed. For any  $x \in \mathbb{B}_r$  and any  $y \in \mathbb{R}^n \setminus \overline{\mathbb{B}_r}$ , the Poisson kernel  $P_r$  is defined by*

$$P_r(x, y) = \alpha(n, s) \left( \frac{r^2 - |x|^2}{|y|^2 - r^2} \right)^s \frac{1}{|x - y|^n}, \quad (2.2)$$

where the constant  $\alpha(n, s)$  is given by

$$\alpha(n, s) = \frac{\Gamma(\frac{n}{2}) \sin(\pi s)}{\pi^{\frac{n}{2}+1}}. \quad (2.3)$$

**Definition 2.2.** ([7]) *Let  $r > 0$  be fixed. For any  $x, y \in \mathbb{B}_r$  and  $x \neq y$ , Green function  $G$  is defined by*

$$G(x, y) = \begin{cases} \kappa(1, \frac{1}{2}) \log \left( \frac{r^2 - xy + \sqrt{(r^2 - x^2)(r^2 - y^2)}}{r|x - y|} \right), & n = 1, \\ \kappa(n, s) |x - y|^{2s-n} \int_0^{r^*(x,y)} \frac{t^{s-1}}{(t+1)^{\frac{n}{2}}} dt, & n \geq 2, \end{cases} \quad (2.4)$$

where

$$r^*(x, y) = \frac{(r^2 - |x|^2)(r^2 - |y|^2)}{r^2|x - y|^2}, \quad (2.5)$$

and  $\kappa(n, s)$  denotes a normalization constant

$$\kappa(n, s) = \begin{cases} \frac{1}{\pi}, & n = 1, \\ \frac{\Gamma(\frac{n}{2})}{2^{2s} \pi^{\frac{n}{2}} \Gamma^2(s)}, & n \geq 2. \end{cases} \quad (2.6)$$

Then the representation formula for (2.1) is stated in the following theorem.

**Theorem 2.1.** ([7]) *Let  $r > 0$ ,  $f \in C^{2s+\varepsilon}(\mathbb{B}_r) \cap C(\overline{\mathbb{B}_r})$  for sufficiently small  $\varepsilon > 0$  and  $g \in L^1_s(\mathbb{R}^n) \cap C(\mathbb{R}^n)$ . Then there exists a unique continuous solution to (2.1) which is given by*

$$u(x) = \int_{\mathbb{R}^n \setminus \mathbb{B}_r} P_r(x, y) g(y) dy + \int_{\mathbb{B}_r} G(x, y) f(y) dy. \quad (2.7)$$

From Theorem 2.1, we can derive the representation formula for problem (1.1) with  $\Omega$  being an arbitrary ball, centered at  $\mathbf{x}_0 \in \mathbb{R}^n$ , namely

$$\begin{cases} (-\Delta)^s u(\mathbf{x}) = f(\mathbf{x}), & \mathbf{x} \in \mathbb{B}_r(\mathbf{x}_0), \\ u(\mathbf{x}) = g(\mathbf{x}), & \mathbf{x} \in \mathbb{R}^n \setminus \mathbb{B}_r(\mathbf{x}_0). \end{cases} \quad (2.8)$$

Through variable translation and replacement, we obtain

$$u(\mathbf{x}) = \int_{\mathbb{R}^n \setminus \mathbb{B}_r(\mathbf{x}_0)} P_r(\mathbf{x} - \mathbf{x}_0, \mathbf{y} - \mathbf{x}_0) g(\mathbf{y}) d\mathbf{y} + \int_{\mathbb{B}_r(\mathbf{x}_0)} G(\mathbf{x} - \mathbf{x}_0, \mathbf{y} - \mathbf{x}_0) f(\mathbf{y}) d\mathbf{y}. \quad (2.9)$$

## 2.2. Numerical method for (2.1) using the Poisson kernel

In this subsection, we first derive the numerical method for the following Dirichlet problem,

$$\begin{cases} (-\Delta)^s u(\mathbf{x}) = 0, & \mathbf{x} \in \mathbb{B}_r, \\ u(\mathbf{x}) = g(\mathbf{x}), & \mathbf{x} \in \mathbb{R}^n \setminus \mathbb{B}_r. \end{cases} \quad (2.10)$$

From Theorem 2.1,

$$u(\mathbf{x}) = \int_{\mathbb{R}^n \setminus \mathbb{B}_r} P_r(\mathbf{x}, \mathbf{y}) g(\mathbf{y}) d\mathbf{y}, \quad (2.11)$$

provided that  $g(\mathbf{x})$  satisfies the condition in Theorem 2.1.

To compute this integral in the above formula, we use change of variables by utilizing the hyperspherical coordinates with radius  $\rho > r$ , angles  $\varphi_1, \varphi_2, \dots, \varphi_{n-2} \in [0, \pi]$ , and  $\theta \in [0, 2\pi]$ . Then, it holds for  $n \geq 3$  that

$$\begin{cases} y_1 = \rho \sin \varphi_1 \sin \varphi_2 \cdots \sin \varphi_{n-2} \sin \theta, \\ y_2 = \rho \sin \varphi_1 \sin \varphi_2 \cdots \sin \varphi_{n-2} \cos \theta, \\ y_3 = \rho \sin \varphi_1 \sin \varphi_2 \cdots \cos \varphi_{n-2}, \\ \dots \\ y_{n-1} = \rho \sin \varphi_1 \cos \varphi_2, \\ y_n = \rho \cos \varphi_1. \end{cases} \quad (2.12)$$

The Jacobian of the transformation is given by  $\rho^{n-1} \sin^{n-2}(\varphi_1) \sin^{n-3}(\varphi_2) \cdots \sin(\varphi_{n-2})$ . Here we discuss the case with  $n \geq 3$ . Two dimensional case can be derived similarly so is omitted here or is left for the interested reader. Without loss of generality and up to rotations, we assume  $\mathbf{x} = e_n = |\mathbf{x}|(0, 0, \dots, 1)$ , so (see Figure 2)

$$|\mathbf{x} - \mathbf{y}|^2 = \rho^2 + |\mathbf{x}|^2 - 2\rho|\mathbf{x}| \cos \varphi_1, \quad n \geq 3. \quad (2.13)$$

Now we have

$$\begin{aligned} u(\mathbf{x}) &= \alpha(n, s) (r^2 - |\mathbf{x}|^2)^s \int_0^\pi \cdots \int_0^{2\pi} \int_r^\infty (\rho^2 - r^2)^{-s} \frac{g(\rho, \theta, \varphi_1, \dots, \varphi_{n-2})}{(\rho^2 + |\mathbf{x}|^2 - 2\rho|\mathbf{x}| \cos \varphi_1)^{\frac{n}{2}}} \\ &\quad \times \rho^{n-1} \sin^{n-2}(\varphi_1) \sin^{n-3}(\varphi_2) \cdots \sin(\varphi_{n-2}) d\rho d\theta d\varphi_1 \cdots d\varphi_{n-2}. \end{aligned} \quad (2.14)$$

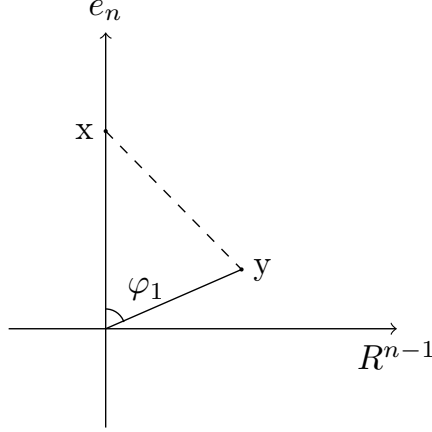


Figure 2: Distance between  $x$  and  $y$ .

To compute the improper integral, we perform the substitution  $\rho = \frac{r}{\rho'}$  and rename  $\rho'$  as  $\rho$ ,

$$u(\mathbf{x}) = \alpha(n, s)(r^2 - |\mathbf{x}|^2)^s r^{n-2s} \int_0^\pi \dots \int_0^{2\pi} \int_0^1 \rho^{2s-1} (1 - \rho^2)^{-s} \frac{g(\frac{r}{\rho}, \theta, \varphi_1, \dots, \varphi_{n-2})}{(r^2 + \rho^2 |\mathbf{x}|^2 - 2r\rho |\mathbf{x}| \cos \varphi_1)^{\frac{n}{2}}} \\ \times \sin^{n-2}(\varphi_1) \sin^{n-3}(\varphi_2) \dots \sin(\varphi_{n-2}) d\rho d\theta d\varphi_1 \dots d\varphi_{n-2}. \quad (2.15)$$

When  $s \in (0, \frac{1}{2})$ , we separate integral into two parts as follows

$$u(\mathbf{x}) = \alpha(n, s)(r^2 - |\mathbf{x}|^2)^s r^{n-2s} \int_0^\pi \dots \int_0^{2\pi} \left( \int_0^{\frac{1}{2}} + \int_{\frac{1}{2}}^1 \right) \rho^{2s-1} (1 - \rho^2)^{-s} \\ \times \frac{g(\frac{r}{\rho}, \theta, \varphi_1, \dots, \varphi_{n-2})}{(r^2 + \rho^2 |\mathbf{x}|^2 - 2r\rho |\mathbf{x}| \cos \varphi_1)^{\frac{n}{2}}} \sin^{n-2}(\varphi_1) \sin^{n-3}(\varphi_2) \dots \sin(\varphi_{n-2}) d\rho d\theta d\varphi_1 \dots d\varphi_{n-2} \\ = c(n, s)(r^2 - |\mathbf{x}|^2)^s r^{n-2s} [I_1(\mathbf{x}) + I_2(\mathbf{x})]. \quad (2.16)$$

Through change of variable  $\rho = \frac{\rho'}{2}$  and  $\theta = 2\pi\theta'$ ,  $\varphi_1 = \pi\varphi'_1, \dots, \varphi_{n-2} = \pi\varphi'_{n-2}$ ,  $I_1(\mathbf{x})$  can be rewritten as

$$I_1(\mathbf{x}) = \pi^{n-1} \int_0^1 \int_0^1 \dots \int_0^1 \left( \frac{\rho'}{2} \right)^{2s-1} \left[ 1 - \left( \frac{\rho'}{2} \right)^2 \right]^{-s} \frac{g(\frac{2r}{\rho'}, 2\pi\theta', \pi\varphi'_1, \dots, \pi\varphi'_{n-2})}{(r^2 + (\frac{\rho'}{2})^2 |\mathbf{x}|^2 - r\rho' |\mathbf{x}| \cos(\pi\varphi'_1))^{\frac{n}{2}}} \\ \times \sin^{n-2}(\pi\varphi'_1) \sin^{n-3}(\pi\varphi'_2) \dots \sin(\pi\varphi'_{n-2}) d\rho' d\theta' d\varphi'_1 \dots d\varphi'_{n-2} \\ = \pi^{n-1} \int_0^1 \int_0^1 \dots \int_0^1 \left( \frac{\rho}{2} \right)^{2s-1} \omega_1(\mathbf{x}, \rho, \theta, \varphi_1, \dots, \varphi_{n-2}) d\rho d\theta d\varphi_1 \dots d\varphi_{n-2}, \quad (2.17)$$

where

$$\omega_1(\mathbf{x}, \rho, \theta, \varphi_1, \dots, \varphi_{n-2}) = \left[ 1 - \left( \frac{\rho}{2} \right)^2 \right]^{-s} \frac{g(\frac{2r}{\rho}, 2\pi\theta, \pi\varphi_1, \dots, \pi\varphi_{n-2})}{(r^2 + (\frac{\rho}{2})^2 |\mathbf{x}|^2 - r\rho |\mathbf{x}| \cos \pi\varphi_1)^{\frac{n}{2}}} \\ \times \sin^{n-2}(\pi\varphi_1) \sin^{n-3}(\pi\varphi_2) \dots \sin(\pi\varphi_{n-2}) \quad (2.18)$$

By the affine transformations  $\rho = \frac{1}{2}\rho' + \frac{1}{2}$  and  $\theta = 2\pi\theta'$ ,  $\varphi_1 = \pi\varphi'_1, \dots, \varphi_{n-2} = \pi\varphi'_{n-2}$ ,  $I_2(\mathbf{x})$  is given by

$$\begin{aligned}
I_2(\mathbf{x}) &= \pi^{n-1} \int_0^1 \dots \int_0^1 \left[ 1 - \left( \frac{\rho' + 1}{2} \right)^2 \right]^{-s} \frac{g\left(\frac{2r}{\rho'+1}, 2\pi\theta', \pi\varphi'_1, \dots, \pi\varphi'_{n-2}\right)}{\left(r^2 + \left(\frac{\rho'+1}{2}\right)^2 |\mathbf{x}|^2 - r(\rho' + 1)|\mathbf{x}| \cos \pi\varphi'_1\right)^{\frac{n}{2}}} \\
&\quad \times \left( \frac{\rho' + 1}{2} \right)^{2s-1} \sin^{n-2}(\pi\varphi'_1) \sin^{n-3}(\pi\varphi'_2) \dots \sin(\pi\varphi'_{n-2}) d\rho' d\theta' d\varphi'_1 \dots d\varphi'_{n-2} \\
&= \pi^{n-1} \int_0^1 \dots \int_0^1 \left( \frac{1-\rho}{2} \right)^{-s} \omega_2(\mathbf{x}, \rho, \theta, \varphi_1, \dots, \varphi_{n-2}) d\rho d\theta d\varphi_1 \dots d\varphi_{n-2},
\end{aligned} \tag{2.19}$$

where

$$\begin{aligned}
\omega_2(\mathbf{x}, \rho, \theta, \varphi_1, \dots, \varphi_{n-2}) &= \left( \frac{3+\rho}{2} \right)^{-s} \left( \frac{\rho+1}{2} \right)^{2s-1} \frac{g\left(\frac{2r}{\rho+1}, 2\pi\theta, \pi\varphi_1, \dots, \pi\varphi_{n-2}\right)}{\left(r^2 + \left(\frac{\rho+1}{2}\right)^2 |\mathbf{x}|^2 - r(\rho+1)|\mathbf{x}| \cos \pi\varphi_1\right)^{\frac{n}{2}}} \\
&\quad \times \sin^{n-2}(\pi\varphi_1) \sin^{n-3}(\pi\varphi_2) \dots \sin(\pi\varphi_{n-2}).
\end{aligned} \tag{2.20}$$

We set the uniform grid  $\{\rho_i\}_{i=1}^N$  for  $\rho$ ,  $\{\theta_j\}_{j=1}^M$  for  $\theta$ ,  $\{(\varphi_m)_{k_m}\}_{k_m=1}^{M_m}$  for  $\varphi_m$ ,  $m = 1, 2, \dots, n-2$ , and  $\{t_k\}_{k=1}^L$  for  $t$ . Here  $\rho_i = ih_\rho$ ,  $\theta_j = jh_\theta$ ,  $(\varphi_m)_{k_m} = k_m h_m$ , and  $t_k = kh_t$  with  $h_\rho = \frac{1}{N}$ ,  $h_\theta = \frac{1}{M}$ ,  $h_m = \frac{1}{M_m}$ , and  $h_t = \frac{1}{L}$ . We also define the interpolation operator by recursive formula,

$$\begin{aligned}
&I_{[\rho_{i-1}, \rho_i]} v(\rho, \theta, \varphi_1, \dots, \varphi_{n-2}) \\
&= \frac{1}{h_\rho} [(\rho_i - \rho)v(\rho_{i-1}, \theta, \varphi_1, \dots, \varphi_{n-2}) + (\rho - \rho_{i-1})v(\rho_i, \theta, \varphi_1, \dots, \varphi_{n-2})], \\
&I_{[\rho_{i-1}, \rho_i] \times [\theta_{j-1}, \theta_j]} v(\rho, \theta, \varphi_1, \dots, \varphi_{n-2}) = I_{[\theta_{j-1}, \theta_j]} I_{[\rho_{i-1}, \rho_i]} v(\rho, \theta, \varphi_1, \dots, \varphi_{n-2}), \\
&\dots \\
&I_{[\rho_{i-1}, \rho_i] \times [\theta_{j-1}, \theta_j] \times [(\varphi_1)_{k_1-1}, (\varphi_1)_{k_1}] \dots \times [(\varphi_{n-2})_{k_{n-2}-1}, (\varphi_{n-2})_{k_{n-2}}]} v(\rho, \theta, \varphi_1, \dots, \varphi_{n-2}) \\
&= I_{[(\varphi_{n-2})_{k_{n-2}-1}, (\varphi_{n-2})_{k_{n-2}}]} I_{[\rho_{i-1}, \rho_i] \times [\theta_{j-1}, \theta_j] \dots \times [(\varphi_{n-3})_{k_{n-3}-1}, (\varphi_{n-3})_{k_{n-3}}]} v(\rho, \theta, \varphi_1, \dots, \varphi_{n-2}).
\end{aligned} \tag{2.21}$$

Then utilizing the interpolation operator to approximate  $\omega_1(\mathbf{x}, \rho, \theta, \varphi_1, \dots, \varphi_{n-2})$  on each



interval yields

$$\begin{aligned}
I_1(\mathbf{x}) &\approx \pi^{n-1} \sum_{i=1}^N \sum_{j=1}^M \sum_{k_1=1}^{M_1} \cdots \sum_{k_{n-2}=1}^{M_{n-2}} \int_{(\varphi_{n-2})_{k_{n-2}-1}}^{(\varphi_{n-2})_{k_{n-2}}} \cdots \int_{(\varphi_1)_{k_1-1}}^{(\varphi_1)_{k_1}} \int_{\theta_{j-1}}^{\theta_j} \int_{\rho_{i-1}}^{\rho_i} \left(\frac{\rho}{2}\right)^{2s-1} \\
&\quad \times I_{[\rho_{i-1}, \rho_i] \times [\theta_{j-1}, \theta_j] \cdots \times [(\varphi_{n-2})_{k_{n-2}-1}, (\varphi_{n-2})_{k_{n-2}}]}[\omega_1(\mathbf{x}, \rho, \theta, \varphi_1, \dots, \varphi_{n-2})] d\rho d\theta d\varphi_1 \cdots d\varphi_{n-2} \\
&= \left(\frac{\pi}{2}\right)^{n-1} \frac{h_\theta \prod_{m=1}^{n-2} h_m}{h_\rho} \sum_{i=1}^N \sum_{j=1}^M \sum_{k_1=1}^{M_1} \cdots \sum_{k_{n-2}=1}^{M_{n-2}} \left\{ \sum_{j'=j-1}^j \sum_{k'_1=k_1-1}^{k_1} \cdots \sum_{k'_{n-2}=k_{n-2}-1}^{k_{n-2}} \right. \\
&\quad \left. [A_1(i)\omega_1(\mathbf{x}, \rho_{i-1}, \theta_{j'}, (\varphi_1)_{k'_1}, \dots, (\varphi_{n-2})_{k'_{n-2}}) + A_2(i)\omega_1(\mathbf{x}, \rho_i, \theta_{j'}, (\varphi_1)_{k'_1}, \dots, (\varphi_{n-2})_{k'_{n-2}})] \right\} \\
&\triangleq I_1^h(\mathbf{x}),
\end{aligned} \tag{2.22}$$

where

$$\begin{cases} A_1(i) = 2^{1-2s} \left[ \frac{\rho_i}{2s} (\rho_i^{2s} - \rho_{i-1}^{2s}) - \frac{1}{2s+1} (\rho_i^{2s+1} - \rho_{i-1}^{2s+1}) \right], \\ A_2(i) = 2^{1-2s} \left[ \frac{1}{2s+1} (\rho_i^{2s+1} - \rho_{i-1}^{2s+1}) + \frac{\rho_{i-1}}{2s} (\rho_i^{2s} - \rho_{i-1}^{2s}) \right]. \end{cases} \tag{2.23}$$

Similarly,  $I_2(\mathbf{x})$  can be approximated as follows,

$$\begin{aligned}
I_2(\mathbf{x}) &\approx \pi^{n-1} \sum_{i=1}^N \sum_{j=1}^M \sum_{k_1=1}^{M_1} \cdots \sum_{k_{n-2}=1}^{M_{n-2}} \int_{(\varphi_{n-2})_{k_{n-2}-1}}^{(\varphi_{n-2})_{k_{n-2}}} \cdots \int_{(\varphi_1)_{k_1-1}}^{(\varphi_1)_{k_1}} \int_{\theta_{j-1}}^{\theta_j} \int_{\rho_{i-1}}^{\rho_i} \left(\frac{1-\rho}{2}\right)^{-s} \\
&\quad \times I_{[\rho_{i-1}, \rho_i] \times [\theta_{j-1}, \theta_j] \cdots \times [(\varphi_{n-2})_{k_{n-2}-1}, (\varphi_{n-2})_{k_{n-2}}]}[\omega_2(\mathbf{x}, \rho, \theta, \varphi_1, \dots, \varphi_{n-2})] d\rho d\theta d\varphi_1 \cdots d\varphi_{n-2} \\
&= \left(\frac{\pi}{2}\right)^{n-1} \frac{h_\theta \prod_{m=1}^{n-2} h_m}{h_\rho} \sum_{i=1}^N \sum_{j=1}^M \sum_{k_1=1}^{M_1} \cdots \sum_{k_{n-2}=1}^{M_{n-2}} \left\{ \sum_{j'=j-1}^j \sum_{k'_1=k_1-1}^{k_1} \cdots \sum_{k'_{n-2}=k_{n-2}-1}^{k_{n-2}} \right. \\
&\quad \left. [B_1(i)\omega_2(\mathbf{x}, \rho_{i-1}, \theta_{j'}, (\varphi_1)_{k'_1}, \dots, (\varphi_{n-2})_{k'_{n-2}}) + B_2(i)\omega_2(\mathbf{x}, \rho_i, \theta_{j'}, (\varphi_1)_{k'_1}, \dots, (\varphi_{n-2})_{k'_{n-2}})] \right\} \\
&\triangleq I_2^h(\mathbf{x}),
\end{aligned} \tag{2.24}$$

where

$$\begin{cases} B_1(i) = 2^s \left\{ \frac{1-\rho_i}{1-s} [(1-\rho_i)^{1-s} - (1-\rho_{i-1})^{1-s}] \right. \\ \quad \left. + \frac{1}{2-s} [(1-\rho_{i-1})^{2-s} - (1-\rho_i)^{2-s}] \right\}, \\ B_2(i) = 2^s \left\{ \frac{1}{2-s} [(1-\rho_i)^{2-s} - (1-\rho_{i-1})^{2-s}] \right. \\ \quad \left. + \frac{1-\rho_{i-1}}{1-s} [(1-\rho_i)^{1-s} - (1-\rho_{i-1})^{1-s}] \right\}. \end{cases} \tag{2.25}$$

Then we derive Scheme I for the approximation of the solution  $u(\mathbf{x})$  when  $s \in (0, \frac{1}{2})$ ,

$$u(\mathbf{x}) \approx c(n, s)(r^2 - |\mathbf{x}|^2)^s r^{n-2s} [I_1^h(\mathbf{x}) + I_2^h(\mathbf{x})] \triangleq u_h(\mathbf{x}). \quad (2.26)$$

When  $s \in [\frac{1}{2}, 1)$ , Scheme I is given as follows,

$$u(\mathbf{x}) \approx \left(\frac{\pi}{2}\right)^{n-1} \frac{h_\theta \prod_{m=1}^{n-2} h_m}{h_\rho} 2^{-s} \alpha(n, s) (r^2 - |\mathbf{x}|^2)^s r^{n-2s} \sum_{i=1}^N \sum_{j=1}^M \sum_{k_1=1}^{M_1} \dots \sum_{k_{n-2}=1}^{M_{n-2}} \left\{ \sum_{j'=j-1}^j \sum_{k'_1=k_1-1}^{k_1} \dots \sum_{k'_{n-2}=k_{n-2}-1}^{k_{n-2}} B_1(i) [\omega_2(\mathbf{x}, 2\rho_{i-1} - 1, \theta_{j'}, (\varphi_1)_{k'_1}, \dots, (\varphi_{n-2})_{k'_{n-2}})] \right. \\ \left. + B_2(i) [\omega_2(\mathbf{x}, 2\rho_i - 1, \theta_{j'}, (\varphi_1)_{k'_1}, \dots, (\varphi_{n-2})_{k'_{n-2}})] \right\}, \quad (2.27)$$

where  $B_1(i)$  and  $B_2(i)$  are defined in equation (2.25).

**Remark 2.1.** The complexity of the quadrature rule is  $\mathcal{O}(NM \prod_{i=1}^{n-2} M_i)$ . Specially, when  $h = h_\rho = h_\theta = h_1 = \dots = h_{n-2} = \frac{1}{N}$ , the complexity is  $\mathcal{O}(N^n)$ .

When the equation has nonconstant source term with homogeneous boundary value, i.e.  $f(\mathbf{x}) \neq 0$  and  $g(\mathbf{x}) = 0$  in equation (2.1), we take the two dimensional case as an example. It follows from

$$u(\mathbf{x}) = \int_{\mathbb{B}_r} G(\mathbf{x}, \mathbf{y}) f(\mathbf{y}) d\mathbf{y} = \kappa(n, s) r^{n-2s} (r^2 - |\mathbf{x}|^2)^s \\ \times \int_0^1 \left( \int_{\mathbb{B}_r \setminus S_h} + \int_{S_h} \right) (r^2 - |\mathbf{y}|^2)^s [(r^2 - |\mathbf{x}|^2)(r^2 - |\mathbf{y}|^2)t + r^2 |\mathbf{x} - \mathbf{y}|^2]^{-1} t^{s-1} f(\mathbf{y}) dt d\mathbf{y} \quad (2.28)$$

in two dimensions that for  $\mathbf{x} = (|\mathbf{x}|, 0) \neq (0, 0)$

$$u(\mathbf{x}) \approx \kappa(n, s) r^{n-2s} (r^2 - |\mathbf{x}|^2)^s \int_0^1 t^{s-1} \left( \int_\phi^{2\pi-\phi} \int_0^r + \int_{-\phi}^\phi \left( \int_0^{\frac{|\mathbf{x}|-h}{\cos\theta}} + \int_{\frac{|\mathbf{x}+h}{\cos\theta}}^r \right) \right) \omega_{31}(\rho, \theta, t) dt d\rho d\theta \\ + \int_0^1 t^{s-1} \left( \int_0^\phi \int_0^{\frac{2h}{\cos\theta}} \omega_{32}(\rho, \theta, t) d\rho d\theta + \int_{-\phi}^0 \int_0^{\frac{2h}{\cos\theta}} \omega_{33}(\rho, \theta, t) d\rho d\theta \right) dt. \quad (2.29)$$

Here  $S_h$  is a square with side length  $h$  centered at  $\mathbf{x}$ ,  $\phi = \arctan \frac{h}{|\mathbf{x}|-h}$  and  $\omega_{31}, \omega_{32}, \omega_{33}$  are integrand in the corresponding fields of Figure 3,

$$\omega_{31}(\rho, \theta, t) = (r^2 - \rho^2)^{2s} \frac{f(\rho \cos \theta, \rho \sin \theta)}{(r^2 - |\mathbf{x}|^2)(r^2 - \rho^2)t + r^2 [(\rho \cos \theta - |\mathbf{x}|)^2 + (\rho \sin \theta)^2]}, \\ \omega_{32}(\rho, \theta, t) = (r^2 - \rho^2)^{2s} \frac{f(\rho \cos \theta + |\mathbf{x}| - h, \rho \sin \theta + h)}{(r^2 - |\mathbf{x}|^2)(r^2 - \rho^2)t + r^2 [(\rho \cos \theta - h)^2 + (\rho \sin \theta + h)^2]}, \\ \omega_{33}(\rho, \theta, t) = (r^2 - \rho^2)^{2s} \frac{f(\rho \cos \theta + |\mathbf{x}| - h, \rho \sin \theta - h)}{(r^2 - |\mathbf{x}|^2)(r^2 - \rho^2)t + r^2 [(\rho \cos \theta - h)^2 + (\rho \sin \theta - h)^2]}. \quad (2.30)$$

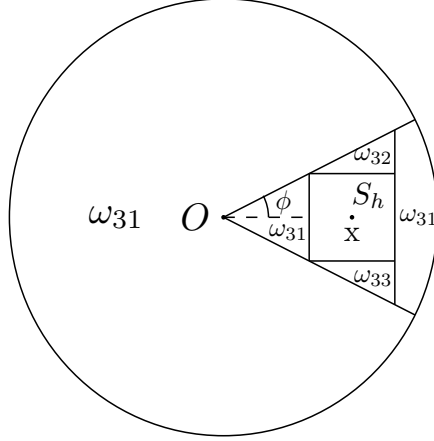


Figure 3: Two dimensional case.

Then we have

$$\begin{aligned}
u_h(\mathbf{x}) = & \kappa(2, s)r^{2-2s}(r^2 - |\mathbf{x}|^2)^s \sum_{i=1}^N \sum_{j=1}^M \sum_{k=1}^L C(k) \left[ (2\pi - 2\phi)r\omega_{31}(r\rho_{i-\frac{1}{2}}, (2\pi - 2\phi)\theta_{j-\frac{1}{2}}, t_{k-\frac{1}{2}}) \right. \\
& + \frac{2\phi(|\mathbf{x}| - h)}{\cos(2\phi\theta_{j-\frac{1}{2}} - \phi)} \omega_{31} \left( \frac{(|\mathbf{x}| - h)\rho_{i-\frac{1}{2}}}{\cos(2\phi\theta_{j-\frac{1}{2}} - \phi)}, 2\phi\theta_{j-\frac{1}{2}} - \phi, t_{k-\frac{1}{2}} \right) + 2\phi \left( r - \frac{|\mathbf{x}| + h}{\cos(2\phi\theta_{j-\frac{1}{2}} - \phi)} \right) \\
& \times \omega_{31} \left( \left( r - \frac{|\mathbf{x}| + h}{\cos(2\phi\theta_{j-\frac{1}{2}} - \phi)} \right) \rho_{i-\frac{1}{2}} + \frac{|\mathbf{x}| + h}{\cos(2\phi\theta_{j-\frac{1}{2}} - \phi)}, 2\phi\theta_{j-\frac{1}{2}} - \phi, t_{k-\frac{1}{2}} \right) \\
& + \frac{2h\phi}{\cos(\phi\theta_{j-\frac{1}{2}})} \omega_{32} \left( \frac{2h\rho_{i-\frac{1}{2}}}{\cos(\phi\theta_{j-\frac{1}{2}})}, \phi\theta_{j-\frac{1}{2}}, t_{k-\frac{1}{2}} \right) \\
& \left. + \frac{2h\phi}{\cos(\phi\theta_{j-\frac{1}{2}} - \phi)} \omega_{33} \left( \frac{2h\rho_{i-\frac{1}{2}}}{\cos(\phi\theta_{j-\frac{1}{2}})}, \phi\theta_{j-\frac{1}{2}} - \phi, t_{k-\frac{1}{2}} \right) \right], \tag{2.31}
\end{aligned}$$

where  $C(k) = \frac{1}{s}(t_k^s - t_{k-1}^s)$ .

When  $\mathbf{x} = (0, 0)$ , we have

$$u_h(\mathbf{x}) = 2\pi(r - h)\kappa(2, s) \sum_{i=1}^N \sum_{j=1}^M \sum_{k=1}^L C(k)\omega_4((r - h)\rho_{i-\frac{1}{2}}, 2\pi\theta_{j-\frac{1}{2}}, t_{k-\frac{1}{2}}), \tag{2.32}$$

where

$$\omega_4(\rho, \theta, t) = (r^2 - \rho^2)^{2s} \frac{f(\rho, \theta)}{(r^2 - \rho^2)t + \rho^2}. \tag{2.33}$$

For higher-dimensional case, the numerical scheme can be similarly derived so is omitted here.

### 2.3. Error estimates of the quadrature rules

In this subsection, we provide error estimates for our numerical method in discretizing the representation formula of the solution  $u(\mathbf{x})$ . Firstly we have the following lemma which can be readily derived.

**Lemma 2.1.** *Let  $I$  be the interpolation operator defined in (2.21) on the domain  $\mathbb{K} = [0, \ell_1] \times [0, \ell_2] \times \dots \times [0, \ell_n]$ . Then for any functions  $v \in C_b^2(\mathbb{K})$ , we have the error estimate,*

$$\|v - Iv\|_{L^\infty} \leq \frac{1}{8} \left( \sum_{i=1}^n \ell_i^2 \left\| \frac{\partial^2 v}{\partial x_i^2} \right\|_{L^\infty} \right). \quad (2.34)$$

In  $n$  ( $n \geq 2$ ) dimensional cases, suppose  $g(x) \in C_b^2(\mathbb{R}^n \setminus \mathbb{B}_r)$ . Then when  $s \in (0, \frac{1}{2})$ , we obtain

$$|u(\mathbf{x}) - u_h(\mathbf{x})| \leq c(n, s)(r^2 - |\mathbf{x}|^2)^s r^{n-2s} [|I_1(\mathbf{x}) - I_1^h(\mathbf{x})| + |I_2(\mathbf{x}) - I_2^h(\mathbf{x})|]. \quad (2.35)$$

From Lemma 2.1 and the fact  $\mathbf{x} \neq \mathbf{y}$ , we derive

$$\begin{aligned} |I_1(\mathbf{x}) - I_1^h(\mathbf{x})| &= \left| \pi^{n-1} \sum_{i=1}^N \sum_{j=1}^M \dots \sum_{k_{n-2}=1}^{M_{n-2}} \int_{(\varphi_{n-2})_{k_{n-2}-1}}^{(\varphi_{n-2})_{k_{n-2}}} \dots \int_{\theta_{j-1}}^{\theta_j} \int_{\rho_{i-1}}^{\rho_i} \left[ \omega_1(\mathbf{x}, \rho, \theta, \varphi_1, \dots, \varphi_{n-2}) \right. \right. \\ &\quad \left. \left. - I_{[\rho_{i-1}, \rho_i] \times [\theta_{j-1}, \theta_j] \times \dots \times [(\varphi_{n-2})_{k_{n-2}-1}, (\varphi_{n-2})_{k_{n-2}}]} \omega_1(\mathbf{x}, \rho, \theta, \varphi_1, \dots, \varphi_{n-2}) \right] \right. \\ &\quad \left. \times \left( \frac{\rho}{2} \right)^{2s-1} d\rho d\theta d\varphi_1 \dots d\varphi_{n-2} \right| \\ &\leq \frac{\pi}{s2^{2s+3}} \left( h_\rho^2 \left\| \frac{\partial^2 \omega_1}{\partial \rho^2} \right\|_{L^\infty} + h_\theta^2 \left\| \frac{\partial^2 \omega_1}{\partial \theta^2} \right\|_{L^\infty} + \sum_{r=1}^{n-2} h_r^2 \left\| \frac{\partial^2 \omega_1}{\partial \varphi_r^2} \right\|_{L^\infty} \right) \\ &\leq C \left( h_\rho^2 + h_\theta^2 + \sum_{r=1}^{n-2} h_r^2 \right). \end{aligned} \quad (2.36)$$

Similarly,

$$|I_2(\mathbf{x}) - I_2^h(\mathbf{x})| \leq C \left( h_\rho^2 + h_\theta^2 + \sum_{r=1}^{n-2} h_r^2 \right). \quad (2.37)$$

When  $s \in [\frac{1}{2}, 1)$ , the truncated errors is still  $\mathcal{O}(h_\rho^2 + h_\theta^2 + \sum_{r=1}^{n-2} h_r^2)$ . Thus we have the theorem as follows.

**Theorem 2.2.** *Let  $r > 0$ ,  $g \in C_b^2(\mathbb{R}^n \setminus \mathbb{B}_r)$  and  $s \in (0, 1)$ . Then it holds that*

$$|u(\mathbf{x}) - u_h(\mathbf{x})| \leq C \left( h_\rho^2 + h_\theta^2 + \sum_{r=1}^{n-2} h_r^2 \right), \quad (2.38)$$

where  $C$  is a positive constant.

When  $f(x) \in C_b^2(\mathbb{B}_r \setminus S_h)$ , it is easily to derive the error estimates for equation (2.31),  $\mathcal{O}(h^{2s} + h_t + h_\rho^2 + h_\theta^2)$ .

Obviously, the above quadrature for  $n$ -dimensional fractional Laplacian is often difficult to be implemented in computer simulations if  $n > 3$ . So the Monte Carlo method is very likely the best choice for numerical experiments. In the following, we introduce modified walk-on-sphere method, which is one of Monte Carlo methods.

### 3. Modified walk-on-sphere method

In this section, we utilize the modified walk-on-sphere method to solve equation (1.1) with  $\Omega$  being an arbitrary domain instead of a ball. Assume  $f(x)$  and  $g(x)$  satisfy the condition in Theorem 2.1. Then it is known from Section 2 that the solution to (1.1),  $u(x_0)$ ,  $x_0 \in \Omega$ , has the integral representation

$$u(x_0) = \int_{\mathbb{R}^n \setminus \mathbb{B}_{r_0}(x_0)} p_{1,r_0}(x, x_0) u(x) dx + a(x_0) \int_{\mathbb{B}_{r_0}(x_0)} p_{2,r_0}(y, x_0) f(y) dy, \quad (3.1)$$

where  $\mathbb{B}_{r_0}(x_0)$  is the largest ball contained in  $\Omega$  with radius  $r_0 = \sup\{r : \mathbb{B}(x_0, r) \subset \Omega\}$ , centered at  $x_0$ ,

$$\begin{cases} p_{1,r_0}(x, x_0) = P_{r_0}(0, x - x_0), \\ p_{2,r_0}(y, x_0) = \frac{1}{a(x_0)} G(0, y - x_0), \end{cases} \quad (3.2)$$

and

$$\left\{ \begin{aligned} a(x_0) &= \int_{\mathbb{B}_{r_0}(x_0)} G(0, y - x_0) dy \\ &= \kappa(n, s) \int_{\mathbb{B}_{r_0}(x_0)} |y - x_0|^{2s-n} \int_0^{\frac{r_0^2 - |y-x_0|^2}{|y-x_0|^2}} \frac{t^{s-1}}{(t+1)^{\frac{n}{2}}} dt dy \\ &= \omega_{n-1} \kappa(n, s) \int_0^{r_0} \rho^{2s-1} \int_0^{\frac{r_0^2 - \rho^2}{\rho^2}} \frac{t^{s-1}}{(t+1)^{\frac{n}{2}}} dt d\rho \\ &= \omega_{n-1} \kappa(n, s) \int_0^\infty \frac{t^{s-1}}{(t+1)^{\frac{n}{2}}} \int_0^{\frac{r_0}{(t+1)^{\frac{1}{2}}}} \rho^{2s-1} d\rho dt \\ &= \kappa(n, s) B(s, \frac{n}{2}) \frac{\omega_{n-1}}{2s} r_0^{2s}. \end{aligned} \right. \quad (3.3)$$

Here  $a(x_0)$  is the normalizing constant such that  $\int_{\mathbb{B}_{r_0}(x_0)} p_{2,r_0}(y, x_0) dy = 1$ . And  $\omega_{n-1}$  denotes the  $(n-1)$ -dimensional measure of the unit sphere  $S^{n-1}$ . We recall from [7] that

$$\int_{\mathbb{R}^n \setminus \mathbb{B}_{r_0}(x_0)} p_{1,r_0}(x, x_0) dx = 1. \quad (3.4)$$

Both  $p_{1,r_0}(x, x_0)$  and  $p_{2,r_0}(y, x_0)$  can be viewed as probability density function for the random variables  $X$  outside the ball  $\mathbb{B}_{r_0}(x_0)$  and  $Y$  inside the ball, respectively. So we can suppose

$X$  and  $Y$  denote random variables outside the ball with density  $p_{1,r_0}(x, x_0)$  and inside the ball with  $p_{2,r_0}(y, x_0)$ , accordingly. Then the integral representation (3.1) can be rewritten as

$$u(x_0) = \mathbb{E}u(X) + a(x_0)\mathbb{E}f(Y). \quad (3.5)$$

Here  $\mathbb{E}$  indicates expected operation. The first term describes a mean value with respect to  $p_{1,r_0}(y, x_0)$  outside the ball and represents the average score upon exiting the ball  $\mathbb{B}_{r_0}(x_0)$ . The second term is a weighted average taken with respect to density  $p_{2,r_0}(x, x_0)$  and represents the expected contribution from sources inside the ball.

Both  $p_{1,r_0}(x, x_0)$  and  $p_{2,r_0}(y, x_0)$  can be used to construct transition probabilities for a Markov chain. The transition from an initial point  $X_0 = x_0$  is performed by selecting a point  $X_1$  outside the ball  $\mathbb{B}_{r_0}(x_0)$  with density  $p_{1,r_0}(x, x_0)$  and by generating a random variable  $Y_1$  with density  $p_{2,r_0}(y, x_0)$ . Given the position  $X_k = x_k$  at the  $k$ -th step, the transition to the  $(k+1)$ -th step is carried out by choosing  $X_{k+1}$  with  $p_{1,r_k}(x, x_k)$ ,  $r_k = \sup\{r : \mathbb{B}(x_k, r) \subset \Omega\}$ , outside the ball  $\mathbb{B}_{r_k}(x_k)$  and by selecting  $Y_{k+1}$  according to the density  $p_{2,r_k}(y, x_k)$  ( $X_{k+1}$  and  $Y_{k+1}$  are independent of each other). The walk on spheres is simulated by repeating this procedure until the particle exits the domain  $\Omega$ . For the point  $X_k$ , the solution  $u(x)$  must satisfy (3.5). We obtain

$$u(X_k) = \mathbb{E}[u(X_{k+1})|X_k] + a(X_k)\mathbb{E}[f(Y_{k+1})|X_k]. \quad (3.6)$$

Here the conditional expectations are used as the densities of  $X_{k+1}$  and  $Y_{k+1}$  are determined by the position of  $X_k$ .

Generally speaking, the connection between the solution to the fractional Laplacian Dirichlet problem and the random process follows from the telescoping summation

$$\begin{aligned} u(x_0) = \mathbb{E}u(X_0) &= \mathbb{E}u(X_l) + \mathbb{E} \left\{ \sum_{k=0}^{l-1} [u(X_k) - u(X_{k+1})] \right\} \\ &= \mathbb{E}u(X_l) + \mathbb{E} \left\{ \sum_{k=0}^{l-1} (u(X_k) - \mathbb{E}[u(X_{k+1})|X_k]) \right\}, \end{aligned} \quad (3.7)$$

where  $X_0 = x_0$ . In the last equality, we have used the fact that

$$\mathbb{E}u(X_{k+1}) = \mathbb{E}\{\mathbb{E}[u(X_{k+1})|X_k]\}. \quad (3.8)$$

Applying identity (3.6) yields

$$\begin{aligned} u(x_0) &= \mathbb{E}u(X_l) + \mathbb{E} \left\{ \sum_{k=0}^{l-1} a(X_k)\mathbb{E}[f(Y_{k+1})|X_k] \right\} \\ &= \mathbb{E}u(X_l) + \mathbb{E} \left[ \sum_{k=0}^{l-1} a(X_k)f(Y_{k+1}) \right]. \end{aligned} \quad (3.9)$$

Now suppose the process jumps out of the boundary on the  $l$ -th step. Then all of the terms on the right-hand side of equation (3.9) would be known and  $u(X_l)$  can be replaced by  $g(X_l)$ .

This suggests that  $u(\mathbf{x}_0)$  be the mean value of the exit points plus a weighted average from internal contribution.

Monte Carlo method makes use of the preceding observation to estimate  $u(\mathbf{x}_0)$ . According to the density  $p_{1,r_k}(\mathbf{x}, \mathbf{x}_k)$ ,  $\mathbf{X}_{k+1}$  will jump out of the ball  $B_{r_k}(\mathbf{x}_k)$  so that the particle will exit the domain in a finite number of steps. At the conclusion of each walk, we compute the random sample

$$Z_i = g(\mathbf{X}_l^i) + \sum_{k=0}^{l-1} a(\mathbf{X}_k^i) f(\mathbf{Y}_{k+1}^i), \quad (3.10)$$

where  $i$  denotes the  $i$ -th experiment. By identity (3.10), we have  $u(\mathbf{x}_0) = \mathbb{E}Z_i$ . An estimate for the mean of  $Z_i$  is given by the statistic

$$S_N = \frac{1}{N} \sum_{i=1}^N Z_i, \quad (3.11)$$

where  $N$  is the number of trials. By the law of large numbers,

$$\lim_{N \rightarrow \infty} S_N = u(\mathbf{x}_0). \quad (3.12)$$

The central limit theorem gives  $\mathcal{O}(1/N)$  upper bounds on the variance of the  $N$ -term sum, which serves as a numerical error estimate.

### 3.1. Modifying the walk-on-sphere method via approximate sampling methods

For the Monte Carlo sampling, we need to sample  $\mathbf{X}_{k+1}$  and  $\mathbf{Y}_{k+1}$  according to their probability density functions. Given the position  $\mathbf{X}_k = \mathbf{x}_k = (x_{k,1}, x_{k,2}, \dots, x_{k,n})$ , we obtain probability measure for  $\mathbf{X}_{k+1}$ ,

$$\begin{aligned} \mathbb{P}_{\mathbf{x}_k}(\mathbf{X}_{k+1} \in d\mathbf{x}) &= p_{1,r_k}(\mathbf{x}, \mathbf{x}_k) d\mathbf{x} = P_{r_k}(0, \mathbf{x} - \mathbf{x}_k) d\mathbf{x}, \quad \mathbf{x} \in \mathbb{R}^n \setminus \mathbb{B}_{r_k}(\mathbf{x}_k) \\ &= c(n, s) \left( \frac{r_k^2}{|\mathbf{x} - \mathbf{x}_k|^2 - r_k^2} \right)^s \frac{1}{|\mathbf{x} - \mathbf{x}_k|^n} d\mathbf{x}. \end{aligned} \quad (3.13)$$

We change variables by using the hyperspherical coordinates with radius  $\rho > r_k$ , angles  $\varphi_1, \varphi_2, \dots, \varphi_{n-2} \in [0, \pi]$ , and  $\theta \in [0, 2\pi]$ . In this case, it holds that

$$\begin{cases} x_1 = x_{k,1} + \rho \sin \varphi_1 \sin \varphi_2 \cdots \sin \varphi_{n-2} \sin \theta, \\ x_2 = x_{k,2} + \rho \sin \varphi_1 \sin \varphi_2 \cdots \sin \varphi_{n-2} \cos \theta, \\ x_3 = x_{k,3} + \rho \sin \varphi_1 \sin \varphi_2 \cdots \cos \varphi_{n-2}, \\ \cdots \\ x_{n-1} = x_{k,n-1} + \rho \sin \varphi_1 \cos \varphi_2, \\ x_n = x_{k,n} + \rho \cos \varphi_1. \end{cases} \quad (3.14)$$

The Jacobian of the transformation is given by  $\rho^{n-1} \sin^{n-2} \varphi_1 \sin^{n-3} \varphi_2 \cdots \sin \varphi_{n-2}$ . Then we derive

$$\begin{aligned} & \mathbb{P}_{x_k}(X_{k+1} \in dx) \\ &= 2 \frac{\pi^{n/2}}{\Gamma(n/2)} c(n, s) r_k^{2s} (\rho^2 - r_k^2)^{-s} \frac{d\rho}{\rho} \times \frac{d\theta}{2\pi} \times \frac{\sin^{n-2} \varphi_1}{I_{n-2}} d\varphi_1 \times \cdots \times \frac{\sin \varphi_{n-2}}{I_1} d\varphi_{n-2}, \end{aligned} \quad (3.15)$$

where  $\rho \geq r_k$ ,

$$I_n = \int_0^\pi \sin^n \varphi d\varphi = \begin{cases} \frac{n-1}{n} \frac{n-3}{n-2} \cdots \frac{1}{2} I_0, & n \text{ is even,} \\ \frac{n-1}{n} \frac{n-3}{n-2} \cdots \frac{1}{2} I_1, & n \text{ is odd,} \end{cases} \quad (3.16)$$

with  $I_0 = \pi$ ,  $I_1 = 2$ , and

$$\prod_{k=1}^{n-2} \int_0^\pi \sin^k \varphi d\varphi = I_1 I_2 \cdots I_{n-2} = \frac{\pi^{n/2-1}}{\Gamma(n/2)}. \quad (3.17)$$

From (3.15), we observe that  $\theta$  is sampled uniformly on  $[0, 2\pi]$ , whereas we can sample the radius  $\rho$  via the inverse transform sampling method [26]. For  $U \sim ([0, 1])$ ,

$$\rho = F^{-1}(U) = r_k (I^{-1}(1 - U; s, 1 - s))^{-1/2}, \quad (3.18)$$

where  $I(x; z, w)$ ,  $z, w > 0$ , is the incomplete beta function

$$I(x; z, w) = \frac{1}{B(z, w)} \int_0^x u^{z-1} (1-u)^{w-1} du, \quad x \in [0, 1]. \quad (3.19)$$

For  $\varphi_1, \varphi_2, \dots, \varphi_{n-2}$ , we use again the inverse transform method to simulate them. Denote  $I_n^*(\phi) = \int_0^\phi \sin^n \varphi d\varphi$  and  $I_n(\phi) = \frac{1}{I_n} I_n^*(\phi)$ ,  $\phi \in [0, \pi]$ . Then we have

$$I_n(\phi) = \frac{1}{I_n} \begin{cases} -\frac{1}{n} \sin^{n-1} \phi \cos \phi + \sum_{i=1}^{n/2-1} -\frac{1}{n-2i} \sin^{n-2i-1} \phi \cos \phi \prod_{j=0}^{i-1} \frac{n-2j-1}{n-2j} \\ + \frac{(n-1)!!}{n!!} I_0^*(\phi), & n \text{ is even,} \\ -\frac{1}{n} \sin^{n-1} \phi \cos \phi + \sum_{i=1}^{(n-1)/2-1} -\frac{1}{n-2i} \sin^{n-2i-1} \phi \cos \phi \prod_{j=0}^{i-1} \frac{n-2j-1}{n-2j} \\ + \frac{(n-1)!!}{n!!} I_1^*(\phi), & n \text{ is odd,} \end{cases} \quad (3.20)$$

where  $I_0^*(\phi) = \phi$ ,  $I_1^*(\phi) = 1 - \cos \phi$ . For random number  $U \sim ([0, 1])$ , we have

$$\varphi_i = I_{n-i-1}^{-1}(U). \quad (3.21)$$



We can readily get  $\varphi_{n-2} = \arccos(1 - 2U)$ ,  $U \sim ([0, 1])$ . When  $i \neq n - 2$ , it is complicated to get the inverse density function and we use rejection sampling method to generate samples  $\varphi_{n-m-1}$  from a target PDF  $\frac{1}{I_m}p(x) = \frac{1}{I_m} \sin^m x$ ,  $m = 2, \dots, n-2$ . The standard RS algorithm [32] allows us to draw samples exactly from the target PDF  $p_0(x)$ .

**Algorithm 3.1** ([32]). *Step 1. Choose an alternative simpler proposal PDF  $q_0(x)$ .  
Step 2. Draw  $x' \sim q_0(x)$  and  $\omega' \sim U([0, 1])$ .  
Step 3. If  $\omega' \leq \frac{p_0(x')}{Kq_0(x')}$ , then  $x'$  is accepted. Otherwise,  $x'$  is discarded.  
Step 4. Repeated steps 2-3 until the desired number of samples has been obtained.*

Since the target PDF for  $\varphi_{n-m-1}$   $p_0(x) = \frac{1}{I_m}p_m(x) = \frac{1}{I_m} \sin^m x$ ,  $m = 2, \dots, n - 2$  is unimodal and symmetric, the proposal PDF is given by truncated Gaussian density,

$$q_0(x) = C_{q,m}q_m(x) = C_{q,m}\beta \exp(-\alpha_m(x - \mu)^2), \quad x \in (0, \pi), \quad (3.22)$$

where the determination of parameters  $\alpha_m, \beta, \mu$  and the normalizing constant  $C_{q,m}$  is in such a way that we obtain a proposal function for applying the rejection sampling method, i.e.  $K = I_m/C_{q,m}$ , such that

$$q_m(x) \geq p_m(x) \quad (3.23)$$

It is easy to get  $\beta = 1, \mu = \frac{\pi}{2}$ . For parameter  $\alpha_m$ , noting that equation (3.23) implies

$$\ln q_m(x) = -\alpha_m(x - \frac{\pi}{2})^2 \geq m \ln \sin(x), \quad (3.24)$$

so

$$\alpha_m \leq -\frac{m \ln \sin(x)}{(x - \frac{\pi}{2})^2}, \quad x \in (0, \pi). \quad (3.25)$$

In order to obtain best positive fit between the proposal and the target, we must set  $\alpha_m = \lim_{x \rightarrow \frac{\pi}{2}} \frac{-m \ln \sin(x)}{(x - \frac{\pi}{2})^2} = \frac{m}{2}$  (see Figure 4). Thus, samples must be drawn from the selected proposal PDF,  $C_{q,m}e^{-\frac{m}{2}(x - \frac{\pi}{2})^2}$ ,  $x \in (0, \pi)$ . For the truncated Gaussians, the technique available in the literature [10] allows us to draw samples efficiently. Finally, the acceptance rate which is the key performance measure for rejection sampling method is

$$\eta = \int_0^\pi \frac{p_m(x)}{q_m(x)} q_0(x) dx = \frac{I_m}{\sqrt{\frac{2\pi}{m}} \operatorname{erf}\left(\sqrt{\frac{2m}{4}}\pi\right)}, \quad (3.26)$$

where  $\operatorname{erf}(x)$  denotes the error function. It is obvious that  $\eta$  is a monotonically increasing function converging to 1 with respect to  $m$  and the acceptance rate is more than 91% (see Figure 4).

Based on the simulation of  $\rho, \theta, \varphi_1, \varphi_2, \dots, \varphi_{n-2}$ , we derive  $\mathbf{x}$  so that the random variable  $X_{k+1}$  can be simulated by  $X_{k+1} = \mathbf{x}$ .

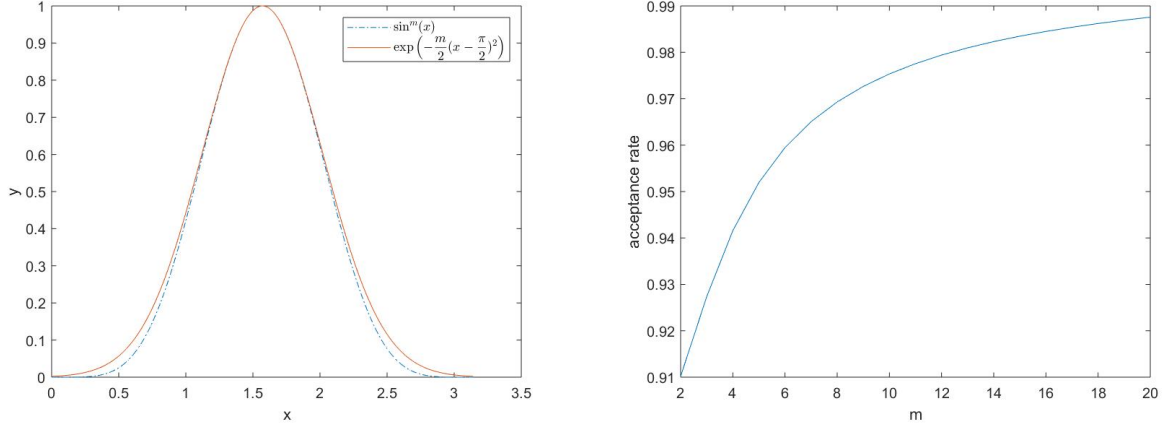


Figure 4: The left figure shows little difference between two functions because of the determination of the parameters. The right figure shows the acceptance rate  $\eta$  converges to 1.

For random variable  $Y_{k+1}$ , it is complicated to sample  $Y_{k+1}$  by using density  $p_{2,r_k}(y, x_k)$ . Thus, we rewrite the second part in (3.1) in the form of

$$\begin{aligned}
& \int_{\mathbb{B}_{r_0}(x_0)} f(y)G(0, y - x_0)dy \\
&= \kappa(n, s) \int_{\mathbb{B}_{r_0}(x_0)} f(y)|y - x_0|^{2s-n} \int_0^{\frac{r_0^2 - |y-x_0|^2}{|y-x_0|^2}} \frac{t^{s-1}}{(t+1)^{\frac{n}{2}}} dt dy.
\end{aligned} \tag{3.27}$$

Performing substitution  $t = \frac{1-t'}{t'}$  yields that

$$\begin{aligned}
& \int_{\mathbb{B}_{r_0}(x_0)} f(y)G(0, y - x_0)dy \\
&= \kappa(n, s) \int_{\mathbb{B}_{r_0}(x_0)} f(y)|y - x_0|^{2s-n} \int_{\frac{|y-x_0|^2}{r_0^2}}^1 (1-t')^{s-1} (t')^{\frac{n}{2}-s-1} dt' dy \\
&= b(x_0) \mathbb{E} \left\{ \left[ 1 - I \left( \frac{|Y - x_0|^2}{r_0^2}; \frac{n}{2} - s, s \right) \right] f(Y) \right\},
\end{aligned} \tag{3.28}$$

where

$$b(x_0) = \kappa(n, s) B\left(\frac{n}{2} - s, s\right) \int_{\mathbb{B}_{r_0}(x_0)} |y - x_0|^{2s-n} dy = \kappa(n, s) B\left(\frac{n}{2} - s, s\right) \frac{r_0^{2s} \pi^{n/2}}{s \Gamma(n/2)} \tag{3.29}$$

and the probability density function for  $Y$  is

$$p_{2,r_0}^*(y, x_0) = \frac{s \Gamma(n/2)}{r_0^{2s} \pi^{n/2}} |y - x_0|^{2s-n}. \tag{3.30}$$

Thus, the equation (3.9) becomes

$$u(\mathbf{x}_0) = \mathbb{E}u(\mathbf{X}_l) + \sum_{k=1}^{l-1} \mathbb{E} \left\{ b(\mathbf{X}_k) \left[ 1 - I \left( \frac{|\mathbf{Y}_{k+1} - \mathbf{X}_k|^2}{r_k^2}; \frac{n}{2} - s, 1 - s \right) \right] f(\mathbf{Y}_{k+1}) \right\}, \quad (3.31)$$

where the random variable  $\mathbf{Y}_{k+1}$  obeys the density  $p_{2,r_k}^*(y, \mathbf{x}_k)$  for the given position  $\mathbf{X}_k = \mathbf{x}_k$ . Using the hyperspherical coordinates (3.14) for PDF and replacing  $\mathbf{x}$  with  $y$  yield

$$\mathbb{P}_{\mathbf{x}_k}(\mathbf{Y}_{k+1} \in dy) = \frac{2s}{r_k^{2s}} \rho^{2s-1} d\rho \times \frac{d\theta}{2\pi} \times \frac{\sin^{n-2} \varphi_1}{I_{n-2}} d\varphi_1 \times \cdots \times \frac{\sin \varphi_{n-2}}{I_1} d\varphi_{n-2}, \quad \rho < r_k. \quad (3.32)$$

Notice that  $\theta \sim U([0, 2\pi])$ ,  $\rho = r_k R^{1/2s}$ , and  $R \sim U([0, 1])$  enable us to simulate  $\theta$  and  $\rho$ . Moreover, we sample  $\varphi_1$  by inverse sample method and  $\varphi_i, i = 2, 3, \dots, n-2$ , by rejection sampling method given before. Then we can simulate  $\mathbf{Y}_{k+1} = y$ .

### 3.2. One-dimensional fractional Poisson equation

When  $n = 1$ , the integral  $I \left( \frac{|\mathbf{Y}_{k+1} - \mathbf{X}_k|^2}{r_k^2}; \frac{1}{2} - s, s \right)$  in (3.27) is infinite if  $\frac{1}{2} < s < 1$ . When  $0 < s < \frac{1}{2}$  and  $n = 1$ , we can still use the method (3.31) with the probability of the moving point's direction  $\theta$  is  $\mathbb{P}\{\theta = +1\} = \mathbb{P}\{\theta = -1\} = \frac{1}{2}$ . To deal with this troublesome integral, we rewrite (3.27) as follows:

$$\begin{aligned} & \int_{x_0-r_0}^{x_0+r_0} f(y)G(0, y - x_0)dy \\ &= \kappa(1, s) \int_{x_0-r_0}^{x_0+r_0} f(y)|y - x_0|^{2s-1} \int_0^{\frac{r_0^2 - |y-x_0|^2}{|y-x_0|^2}} \frac{t^{s-1}}{(t+1)^{\frac{1}{2}}} dt dy \\ &= \kappa(1, s) \int_0^{r_0} [f(x_0 + \rho) + f(x_0 - \rho)] \rho^{2s-1} \int_0^{\frac{r_0^2 - \rho^2}{\rho^2}} \frac{t^{s-1}}{(t+1)^{\frac{1}{2}}} dt d\rho \\ &= 2\kappa(1, s) \int_0^{r_0} \mathbb{E}_\theta[f(x_0 + \rho\theta)] \rho^{2s-1} \int_0^{\frac{r_0^2 - \rho^2}{\rho^2}} \frac{t^{s-1}}{(t+1)^{\frac{1}{2}}} dt d\rho, \end{aligned} \quad (3.33)$$

where we perform substitution  $\rho = |y - x_0|$  and  $\theta$  denotes the random variable with  $\mathbb{P}\{\theta = +1\} = \mathbb{P}\{\theta = -1\} = \frac{1}{2}$ . Via a change of variable  $t' = \rho^2 t$  for the inner integral, we obtain

$$\int_0^{r_0^2 - \rho^2} \left( \frac{t'}{\rho^2} \right)^{s-1} \left( \frac{t'}{\rho^2} + 1 \right)^{-\frac{1}{2}} d \frac{t'}{\rho^2} = \rho^{1-2s} \int_0^{r_0^2 - \rho^2} t'^{s-1} (t' + \rho^2)^{-\frac{1}{2}} dt'. \quad (3.34)$$

It follows from (3.33) that

$$\begin{aligned}
& 2\kappa(1, s) \int_0^{r_0} \mathbb{E}_\theta[f(x_0 + \rho\theta)] \int_0^{r_0^2 - \rho^2} t^{s-1}(t + \rho^2)^{-\frac{1}{2}} dt d\rho \\
&= 2r_0\kappa(1, s) \mathbb{E}_\rho \left\{ \mathbb{E}_\theta[f(x_0 + \rho\theta)] \int_0^{r_0^2 - \rho^2} t^{s-1}(t + \rho^2)^{-\frac{1}{2}} dt \right\} \\
&= 2r_0\kappa(1, s) \mathbb{E}_Y \left[ f(Y) \int_0^{r_0^2 - |Y - x_0|^2} t^{s-1}(t + |Y - x_0|^2)^{-\frac{1}{2}} dt \right]
\end{aligned} \tag{3.35}$$

where  $Y = x_0 + \rho\theta$  with  $\rho \sim U([0, r_0])$  and  $\mathbb{P}\{\theta = +1\} = \mathbb{P}\{\theta = -1\} = \frac{1}{2}$ . Then we show that the integral in the expectation can be represented by the hypergeometric function. For simplicity, let  $a = |Y - x_0|^2$  and  $b = r_0^2 - a$ . We obtain

$$\begin{aligned}
& \int_0^b t^{s-1}(t + a)^{-\frac{1}{2}} dt = \int_0^1 (bt)^{s-1}(a + bt)^{-\frac{1}{2}} dbt \\
&= a^{-\frac{1}{2}} b^s \int_0^1 t^{s-1} \left(1 + \frac{b}{a}t\right)^{-\frac{1}{2}} dt \\
&= a^{-\frac{1}{2}} b^s \left[ \int_0^1 t^{s-1} \left(1 + \frac{b}{a}t\right)^{\frac{1}{2}} dt - \frac{b}{a} \int_0^1 t^s \left(1 + \frac{b}{a}t\right)^{-\frac{1}{2}} dt \right] \\
&= \frac{a^{-\frac{3}{2}} b^s}{s(s+1)} \left[ a(s+1) {}_2F_1\left(-0.5, s; s+1; -\frac{b}{a}\right) - bs {}_2F_1\left(0.5, s+1; s+2; -\frac{b}{a}\right) \right],
\end{aligned} \tag{3.36}$$

where  ${}_2F_1(b, c; d; z)$  is the hypergeometric function given by the analytic continuation

$${}_2F_1(a, b, c; x) = \frac{\Gamma(c)}{\Gamma(b)\Gamma(c-b)} \int_0^1 t^{b-1}(1-t)^{c-b-1}(1-tx)^{-a} dt. \tag{3.37}$$

Finally, equation (3.9) can be changed into

$$\begin{aligned}
u(x_0) &= \mathbb{E}u(X_l) + 2\kappa(1, s) \sum_{k=1}^{l-1} \mathbb{E} \left\{ r_k f(Y_{k+1}) \int_0^{r_k^2 - |Y_{k+1} - X_k|^2} t^{s-1}(t + |Y_{k+1} - X_k|^2)^{-\frac{1}{2}} dt \right\} \\
&= \mathbb{E}u(X_l) + 2\kappa(1, s) \sum_{k=1}^{l-1} \mathbb{E} \left\{ r_k f(Y_{k+1}) \frac{1}{|Y_{k+1} - X_k|^3 s(s+1)} \right. \\
&\quad \times \left[ |Y_{k+1} - X_k|^2 (s+1) {}_2F_1\left(-0.5, s; s+1; \frac{r_k^2 - |Y_{k+1} - X_k|^2}{|Y_{k+1} - X_k|^2}\right) \right. \\
&\quad \left. \left. - (r_k^2 - |Y_{k+1} - X_k|^2) s {}_2F_1\left(0.5, s+1; s+2; \frac{r_k^2 - |Y_{k+1} - X_k|^2}{|Y_{k+1} - X_k|^2}\right) \right] \right\}.
\end{aligned} \tag{3.38}$$

When  $n = 2s$ , i.e.,  $s = \frac{1}{2}$ , we have

$$u(\mathbf{x}_0) = \mathbb{E}u(X_l) + 2\kappa(1, \frac{1}{2}) \sum_{k=1}^{l-1} \mathbb{E} \left\{ r_k f(Y_{k+1}) \log \left( \frac{r_k + \sqrt{r_k^2 - |Y_{k+1} - X_k|^2}}{|Y_{k+1} - X_k|} \right) \right\}. \quad (3.39)$$

Here,  $Y_{k+1} = x_k + \rho\theta$  with  $\rho \sim U(0, r_k)$  and  $\mathbb{P}\{\theta = 1\} = \mathbb{P}\{\theta = -1\} = \frac{1}{2}$ . And the random variable  $X_k$ ,  $k = 1, 2, \dots, l$  can be derived by the method introduced in high dimension which will undergo a long jump.

### 3.3. Summary of the modified walk-one-spheres method

We summarize the method in the following algorithm for equation (1.1),  $n \geq 2$ :

**Algorithm 3.2.** Assign fractional order  $s$ , the domain  $\Omega$ , the point  $\mathbf{x}_0 \in \mathbb{R}^n$ , and the number of samples  $N$ .

*Step 1.* Sample  $X_1$  and  $Y_1$  by probability density functions  $p_{1,r_0}(\mathbf{x}, \mathbf{x}_0)$  in (3.13) and  $p_{2,r_0}^*(y, \mathbf{x}_0)$  in (3.30) based on  $X_0 = \mathbf{x}_0$ , respectively.

*Step 2.* If the latest  $X_k$  is out of  $\Omega$ , go to Step 4. Otherwise, go to Step 3.

*Step 3.* Sample  $X_{k+1}$  and  $Y_{k+1}$  by probability density functions  $p_{1,r_k}(\mathbf{x}, \mathbf{x}_k)$  in (3.13) and  $p_{2,r_k}^*(y, \mathbf{x}_k)$  in (3.30) based on  $X_k = \mathbf{x}_k$ , respectively and go back to Step 2.

*Step 4.* Calculate  $u(x) = g(X_n) + \sum_{k=0}^{l-1} \mathbb{E} \left\{ b(X_k) \left[ 1 - I \left( \frac{|Y_{k+1} - X_k|^2}{r_k^2}; \frac{n}{2} - s, 1 - s \right) \right] f(Y_{k+1}) \right\}$ .

*Step 5.* Implement Step 1-4 for  $N$  times. Then calculate  $u(\mathbf{x}) \approx \frac{1}{N} \sum_{i=1}^N u^i(\mathbf{x})$ .

## 4. Bounds on expected steps of walks on spheres

In the section, we focus on the problem (2.1) when the dimensionality  $n \geq 2$ . We give the upper bound on the number of steps  $l$  in expectation as follows.

**Theorem 4.1.** Consider the problem (2.1) when  $n \geq 2$ . For random walks originating at  $\mathbf{x}_0 \in \mathbb{B}_r$ , the expectation of the number of steps  $l$  in Algorithm 3.2 is

$$\begin{aligned} \mathbb{E}(l) &\leq 2^{4s+1} \pi^{\frac{n}{2}} \frac{\Gamma(s + \frac{n}{2}) \Gamma(s + 1)}{\Gamma^2(\frac{n}{2})} C_4(n, s) \left\{ \frac{2^s}{s_1} + (r - |\mathbf{x}_0|)^s \right. \\ &\quad \times \left[ r^{n - \frac{1+s_1+s}{2}} B \left( 1 - \frac{1+s_1+s}{2}, n \right) \right]^{\frac{2(s_1+s)}{1+s_1+s}} \left( \frac{1}{\frac{(1+s_1+s)(s_1-n)}{1-s_1-s} + n} \right. \\ &\quad \left. \left. \times \left[ (r + |\mathbf{x}_0|)^{\frac{(1+s_1+s)(s_1-n)}{1-s_1-s} + n} - \left( \frac{r - |\mathbf{x}_0|}{2} \right)^{\frac{(1+s_1+s)(s_1-n)}{1-s_1-s} + n} \right]^{\frac{1-s_1-s}{1+s_1+s}} \right) \right\}, \end{aligned} \quad (4.1)$$

where  $s_1 = s$ ,  $s \in (0, \frac{1}{3}]$  and  $s_1 = \frac{1-s}{2}$ ,  $s \in (\frac{1}{3}, 1)$ . The right-hand-side function is increasing with respect to  $s$  and  $|\mathbf{x}_0|$ , respectively.

Before the proof of Theorem 4.1, we need to introduce following lemmas. Observe that the number of walks  $l$  depends only on the domain  $\Omega$  and is independent of  $f(x)$  and  $g(x)$ . Thus we may consider the problem, for fixed  $r > 0$ , given by

$$\begin{cases} (-\Delta)^s u(x) = f(x), & x \in \mathbb{B}_r, \\ u(x) = 0, & x \in \mathbb{R}^n \setminus \mathbb{B}_r, \end{cases} \quad (4.2)$$

where  $s \in (0, 1)$  and  $f(x) = (d(x))^{-2s}$  and  $d(x) = r - |x|$  denotes the minimum distance from  $x$  to the boundary  $\partial\mathbb{B}_r$ . For any  $x_k \in \mathbb{B}_r$ ,  $d(x_k) = r_k$ .

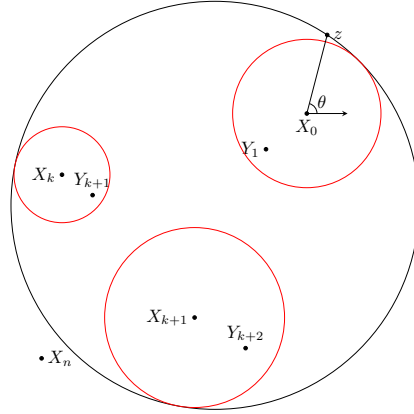


Figure 5: Diagram for expected stopping steps.  $X_n$  is the stopping point.

Recall that the Green function  $G_{\mathbb{B}_r}(x, y)$  in Section 1 is given by

$$G_{\mathbb{B}_r}(x, y) = 2^{-2s} \pi^{-n/2} \Gamma(s)^{-2} \Gamma\left(\frac{n}{2}\right) |x - y|^{2s-n} \int_0^{r^*(x,y)} \frac{t^{s-1}}{(t+1)^{\frac{n}{2}}} dt. \quad (4.3)$$

**Lemma 4.1.** ([9]) *For any ball centred at the origin,  $\mathbb{B}_r \subset \mathbb{R}^n$ , we have*

$$G_{\mathbb{B}_r}(x, y) \leq C_1(n, s) \frac{(d(x))^s (d(y))^s}{|x - y|^n}, \quad x, y \in \mathbb{B}_r, \quad (4.4)$$

where  $C_1(n, s) = \pi^{-n/2} \Gamma(s)^{-1} \Gamma(s+1)^{-1} \Gamma(\frac{n}{2})$ .

**Lemma 4.2.** ([9]) *For any ball centred at the origin,  $\mathbb{B}_r \subset \mathbb{R}^n$ , we have*

$$G_{\mathbb{B}_r}(x, y) \leq C_3(n, s) \frac{(d(x))^s}{(d(y))^s |x - y|^{n-2s}}, \quad x, y \in \mathbb{B}_r, \quad (4.5)$$

where  $C_3(n, s) = 2^{2s} \max\{C_1(n, s), C_2(n, s)\}$  and  $C_2(n, s) = 2^{-2s} \pi^{-n/2} \Gamma(\frac{n}{2} - s) \Gamma(s)^{-1}$ .

Then we have the result in the following.

**Lemma 4.3.** For any ball centred at the origin,  $\mathbb{B}_r \subset \mathbb{R}^n$ , and  $s_1 \in (0, 2s)$ ,

$$G_{\mathbb{B}_r}(\mathbf{x}, \mathbf{y}) \leq C_4(n, s)(d(\mathbf{x}))^s \frac{(d(\mathbf{y}))^{s-s_1}}{|\mathbf{x} - \mathbf{y}|^{n-s_1}}, \quad \mathbf{x}, \mathbf{y} \in \mathbb{B}_r, \quad (4.6)$$

where  $C_4(n, s) = \pi^{-n/2} \Gamma(s)^{-1} \max \left\{ \frac{2^{2s} \Gamma(\frac{n}{2})}{\Gamma(1+s)}, \Gamma(\frac{n}{2} - s) \right\}$ .

*Proof.* Clearly, Lemma 4.3 holds for  $\mathbf{x} = \mathbf{y}$ . For  $\mathbf{x}, \mathbf{y} \in \mathbb{B}_r$ , by Lemmas 4.1 and 4.2, we obtain

$$\begin{aligned} G_{\mathbb{B}_r}(\mathbf{x}, \mathbf{y}) &\leq \left[ C_1(n, s) \frac{(d(\mathbf{x}))^s (d(\mathbf{y}))^s}{|\mathbf{x} - \mathbf{y}|^n} \right] \wedge \left[ C_3(n, s) \frac{(d(\mathbf{x}))^s}{(d(\mathbf{y}))^s |\mathbf{x} - \mathbf{y}|^{n-2s}} \right] \\ &\leq \max\{C_1(n, s), C_3(n, s)\} (d(\mathbf{x}))^s \frac{(d(\mathbf{y}))^{s-s_1}}{|\mathbf{x} - \mathbf{y}|^{n-s_1}} \left\{ \left( \frac{d(\mathbf{y})}{|\mathbf{x} - \mathbf{y}|} \right)^{s_1} \wedge \left( \frac{|\mathbf{x} - \mathbf{y}|}{d(\mathbf{y})} \right)^{2s-s_1} \right\} \\ &\leq C_4(n, s)(d(\mathbf{x}))^s \frac{(d(\mathbf{y}))^{s-s_1}}{|\mathbf{x} - \mathbf{y}|^{n-s_1}}, \end{aligned} \quad (4.7)$$

where  $a \wedge b = \min\{a, b\}$  and

$$\begin{aligned} C_4(n, s) &= \max \{ C_1(n, s), 2^{2s} \max\{C_1(n, s), C_2(n, s)\} \} = 2^{2s} \max\{C_1(n, s), C_2(n, s)\} \\ &= \pi^{-n/2} \Gamma(s)^{-1} \max \left\{ \frac{2^{2s} \Gamma(\frac{n}{2})}{\Gamma(1+s)}, \Gamma\left(\frac{n}{2} - s\right) \right\}. \end{aligned} \quad (4.8)$$

□

*Proof of Theorem 4.1.* From Lemma 4.3 we know that  $\int_{\mathbb{B}_r} f(\mathbf{y})G(\mathbf{x}_0, \mathbf{y})d\mathbf{y}$  with  $\mathbf{x}_0 \in \mathbb{B}_r$  is finite and is the solution to problem (4.2), i.e.,

$$u(\mathbf{x}_0) = \int_{\mathbb{B}_r} f(\mathbf{y})G(\mathbf{x}_0, \mathbf{y})d\mathbf{y}, \quad \mathbf{x}_0 \in \mathbb{B}_r. \quad (4.9)$$

By using equation (3.9), we derive

$$\begin{aligned} u(\mathbf{x}_0) &= \int_{\mathbb{B}_r} f(\mathbf{y})G(\mathbf{x}_0, \mathbf{y})d\mathbf{y} = \mathbb{E}g(X_l) + \mathbb{E} \left[ \sum_{k=0}^{l-1} a(\mathbf{x}_k) f(\mathbf{Y}_{k+1}) \right] \\ &= \mathbb{E} \left[ \sum_{k=0}^{l-1} a(\mathbf{X}_k) f(\mathbf{Y}_{k+1}) \right], \end{aligned} \quad (4.10)$$

where  $\mathbb{E}u(\mathbf{X}_l) = \mathbb{E}g(\mathbf{X}_l) = 0$  have been used since  $\mathbf{X}_l$  is in the outside of the ball. For  $k = 0, 1, \dots, l-1$ , recalling

$$a(\mathbf{X}_k) = \kappa(n, s) B(s, \frac{n}{2}) \frac{\omega_{n-1}}{2s} d(\mathbf{X}_k)^{2s}, \quad (4.11)$$

the definition of  $f(x) = (d(x))^{-2s}$  in equation (4.2) and the fact that  $d(Y_{k+1}) \leq 2d(X_k)$  (see Figure 5) lead to the lower bound

$$a(X_k)f(Y_{k+1}) = \kappa(n, s)B\left(s, \frac{n}{2}\right) \frac{\omega_{n-1}}{2s} \left[\frac{d(X_k)}{d(Y_{k+1})}\right]^{2s} \geq \kappa(n, s)B\left(s, \frac{n}{2}\right) \frac{\omega_{n-1}}{2s} \left(\frac{1}{2}\right)^{2s}. \quad (4.12)$$

Then we have

$$\kappa(n, s)B\left(s, \frac{n}{2}\right) \frac{\omega_{n-1}}{2s} \left(\frac{1}{2}\right)^{2s} \mathbb{E}(l) \leq \int_{\mathbb{B}_r} f(y)G(x_0, y)dy. \quad (4.13)$$

For the right hand side of the inequality, we utilize Lemma 4.3 and partition domain  $B_r$  into two parts,

$$\begin{aligned} \int_{\mathbb{B}_r} f(y)G(x_0, y)dy &= \kappa(n, s) \int_{\mathbb{B}_r} f(y)|y - x_0|^{2s-n} \int_0^{r^*(x_0, y)} \frac{t^{s-1}}{(t+1)^{\frac{n}{2}}} dt dy \\ &\leq C_4(n, s)(d(x_0))^s \int_{\mathbb{B}_r} f(y) \frac{(d(y))^{s-s_1}}{|x_0 - y|^{n-s_1}} dy \\ &= C_4(n, s)(d(x_0))^s \left[ \int_{\mathbb{B}_h(x_0)} + \int_{\mathbb{B}_r \setminus \mathbb{B}_h(x_0)} \right] f(y) \frac{(d(y))^{s-s_1}}{|x_0 - y|^{n-s_1}} dy \\ &= C_4(n, s)(d(x_0))^s [I_1 + I_2], \end{aligned} \quad (4.14)$$

where we set  $h = \frac{r-|x_0|}{2}$ ,  $s_1 = s$ ,  $s \in (0, \frac{1}{3}]$  and  $s_1 = \frac{1-s}{2}$ ,  $s \in (\frac{1}{3}, 1)$ . For  $I_1$ , we obtain

$$\begin{aligned} I_1 &= \int_{\mathbb{B}_h(x_0)} (d(y))^{-s-s_1} |y - x_0|^{s_1-n} dy \\ &\leq (r - |x_0| - h)^{-s-s_1} \int_{\mathbb{B}_h(x_0)} |y - x_0|^{s_1-n} dy \\ &= (r - |x_0| - h)^{-s-s_1} \frac{\omega_{n-1}}{s_1} h^{s_1} \\ &= \frac{2^s \omega_{n-1}}{s_1} (r - |x_0|)^{-s}. \end{aligned} \quad (4.15)$$

For  $I_2$ , we have

$$\begin{aligned} I_2 &= \int_{\mathbb{B}_r \setminus \mathbb{B}_h(x_0)} d(y)^{-s-s_1} |x_0 - y|^{s_1-n} dy \\ &\leq \left( \int_{\mathbb{B}_r \setminus \mathbb{B}_h(x_0)} [d(y)^{-s-s_1}]^{\frac{1+s_1+s}{2(s+s_1)}} dy \right)^{\frac{2(s+s_1)}{1+s_1+s}} \left( \int_{\mathbb{B}_r \setminus \mathbb{B}_h(x_0)} (|x_0 - y|^{s_1-n})^{\frac{1+s_1+s}{1-s_1-s}} dy \right)^{\frac{1-s_1-s}{1+s_1+s}} \\ &= (I_{2,1})^{\frac{2(s_1+s)}{1+s_1+s}} (I_{2,2})^{\frac{1-s_1-s}{1+s_1+s}}. \end{aligned} \quad (4.16)$$



For  $I_{2,1}$ , we use the polar coordinates, hence

$$\begin{aligned}
I_{2,1} &\leq \omega_{n-1} \int_0^r (r-\rho)^{-\frac{1+s_1+s}{2}} \rho^{n-1} d\rho \\
&= \omega_{n-1} r^{n-\frac{1+s_1+s}{2}} \int_0^1 (1-\rho)^{\frac{1+s_1+s}{2}} \rho^{n-1} d\rho \\
&= \omega_{n-1} r^{n-\frac{1+s_1+s}{2}} B\left(1 - \frac{1+s_1+s}{2}, n\right).
\end{aligned} \tag{4.17}$$

For  $I_{2,2}$ , we use polar coordinates  $(\rho, \theta)$  with  $x_0$  being treated as the origin. Let us consider a ray that originates from  $x_0$  and has angle  $\theta$ , which intersect  $\partial\mathbb{B}_r$  on  $z$  (see Figure 5). Then we define  $r(\theta) = |z - x_0|$  and the integral  $I_{2,2}$  can be rewritten as

$$\begin{aligned}
I_{2,2} &= \int_{\mathbb{B}_r \setminus \mathbb{B}_h(x_0)} |x_0 - y|^{\frac{(1+s_1+s)(s_1-n)}{1-s_1-s}} dy \\
&= \omega_{n-1} \int_h^{r(\theta)} \rho^{\frac{(1+s_1+s)(s_1-n)}{1-s_1-s} + n - 1} d\rho \\
&\leq \frac{\omega_{n-1}}{\frac{(1+s_1+s)(s_1-n)}{1-s_1-s} + n} \left[ (r + |x_0|)^{\frac{(1+s_1+s)(s_1-n)}{1-s_1-s} + n} - \left(\frac{r - |x_0|}{2}\right)^{\frac{(1+s_1+s)(s_1-n)}{1-s_1-s} + n} \right]
\end{aligned} \tag{4.18}$$

Bringing (4.14), (4.15), and (4.16) into inequality (4.13) and noticing  $\kappa(n, s) > 0$  yield that

$$\begin{aligned}
&\kappa(n, s) B\left(s, \frac{n}{2}\right) \frac{\omega_{n-1}}{2s} \left(\frac{1}{2}\right)^{2s} \mathbb{E}(l) \\
&\leq C_4(n, s) (r - |x_0|)^s \left\{ \frac{2^s \omega_{n-1}}{s_1} (r - |x_0|)^{-s} + \left[ \omega_{n-1} r^{n-\frac{1+s_1+s}{2}} B\left(1 - \frac{1+s_1+s}{2}, n\right) \right]^{\frac{2(s_1+s)}{1+s_1+s}} \right. \\
&\quad \left. \times \left( \frac{\omega_{n-1}}{\frac{(1+s_1+s)(s_1-n)}{1-s_1-s} + n} \left[ (r + |x_0|)^{\frac{(1+s_1+s)(s_1-n)}{1-s_1-s} + n} - \left(\frac{r - |x_0|}{2}\right)^{\frac{(1+s_1+s)(s_1-n)}{1-s_1-s} + n} \right] \right)^{\frac{1-s_1-s}{1+s_1+s}} \right\}.
\end{aligned}$$

Thus, we arrive at the following estimate:

$$\begin{aligned}
\mathbb{E}(l) &\leq 2^{4s+1} \pi^{\frac{n}{2}} \frac{\Gamma(s + \frac{n}{2}) \Gamma(s+1)}{\Gamma^2(\frac{n}{2})} C_4(n, s) \left\{ \frac{2^s}{s_1} + (r - |x_0|)^s \right. \\
&\quad \times \left[ r^{n-\frac{1+s_1+s}{2}} B\left(1 - \frac{1+s_1+s}{2}, n\right) \right]^{\frac{2(s_1+s)}{1+s_1+s}} \left( \frac{1}{\frac{(1+s_1+s)(s_1-n)}{1-s_1-s} + n} \right. \\
&\quad \left. \left. \times \left[ (r + |x_0|)^{\frac{(1+s_1+s)(s_1-n)}{1-s_1-s} + n} - \left(\frac{r - |x_0|}{2}\right)^{\frac{(1+s_1+s)(s_1-n)}{1-s_1-s} + n} \right] \right)^{\frac{1-s_1-s}{1+s_1+s}} \right\}.
\end{aligned} \tag{4.19}$$

Here  $s_1 = s$ , for  $s \in (0, \frac{1}{3}]$  and  $s_1 = \frac{1-s}{2}$  for  $s \in (\frac{1}{3}, 1)$ . So inequality (4.1) is shown.

We are now in position to bound the expected number of steps  $l$  before stopping. Let  $a(s) = -\left[\frac{(1+s_1+s)(s_1-n)}{1-s_1-s} + n\right] = \frac{s^2+4ns+2s+4n-3}{2(1-s)}$  and  $\rho = \frac{|x_0|}{r}$ . Then, for  $s \in (\frac{1}{3}, 1)$ , we have

$$\begin{aligned} \mathbb{E}(l) \leq \max\{C_5(n, s), C_6(n, s)\} & \left\{ \frac{2^{s+1}}{1-s} + (1-\rho)^s \left[ B\left(\frac{1-s}{4}, 2\right) \right]^{\frac{2+2s}{3+s}} \right. \\ & \left. \times \left( -\frac{1}{a(s)} \left[ (1+\rho)^{-a(s)} - 2^{a(s)}(1-\rho)^{-a(s)} \right] \right)^{\frac{1-s}{3+s}} \right\}, \end{aligned} \quad (4.20)$$

where

$$\begin{aligned} C_5(n, s) &= \frac{2^{6s+1}}{B\left(s, \frac{n}{2}\right)}, \\ C_6(n, s) &= 2^{4s+1} s \frac{\Gamma\left(s + \frac{n}{2}\right) \Gamma\left(\frac{n}{2} - s\right)}{\Gamma^2\left(\frac{n}{2}\right)}. \end{aligned} \quad (4.21)$$

Let  $v(s, \rho)$  be the right hand side of equation (4.20). Since we have

$$\begin{aligned} & (1-\rho)^s \left( -\frac{1}{a(s)} \left[ (1+\rho)^{-a(s)} - 2^{a(s)}(1-\rho)^{-a(s)} \right] \right)^{\frac{1-s}{3+s}} \\ &= \left( \frac{1}{a(s)} \right)^{\frac{1-s}{3+s}} \left[ 2^{a(s)}(1-\rho)^{\frac{s(3+s)}{1-s}-a(s)} - (1+\rho)^{-a(s)}(1-\rho)^{\frac{s(3+s)}{1-s}} \right]^{\frac{1-s}{3+s}} \end{aligned} \quad (4.22)$$

and  $\frac{s(3+s)}{1-s} - a(s) < 0$ , it can be readily checked that  $v(s, \rho)$  is a monotonically increasing function with respect to  $\rho$  so that we discuss monotonicity for  $s$ . For  $C_5(n, s)$ , it is easily obtain  $C_5(n, s)$  monotonically increases with respect to  $s$ . Observe that  $C_6(n, s)$  can be written as follows.

$$C_6(n, s) = 2^{4s+1} s B\left(\frac{n}{2} + s, \frac{n}{2} - s\right) \frac{\Gamma(n)}{\Gamma^2\left(\frac{n}{2}\right)}. \quad (4.23)$$

Differentiating Beta function with respect to  $s$ , we obtain

$$\begin{aligned} B'\left(\frac{n}{2} + s, \frac{n}{2} - s\right) &= \int_0^1 x^{s+\frac{n}{2}-1} (1-x)^{\frac{n}{2}-s-1} \ln\left(\frac{x}{1-x}\right) dx \\ &= \int_0^{\frac{1}{2}} x^{\frac{n}{2}-s-1} (1-x)^{\frac{n}{2}-s-1} \left[ x^{2s} \ln\left(\frac{x}{1-x}\right) + (1-x)^{2s} \ln\left(\frac{1-x}{x}\right) \right] dx. \end{aligned} \quad (4.24)$$

Since the integrand in the square bracket is nonnegative,  $B\left(\frac{n}{2} + s, \frac{n}{2} - s\right)$  increases monotonically such that both  $C_6(n, s)$  and  $\max\{C_5(n, s), C_6(n, s)\}$  are monotonically increasing coefficients. Then we discuss the second term in the brace of the equation (4.20), which is

denoted by  $v_1(s, \rho)$ . Taking logarithm of  $v_1(s, \rho)$  yields

$$\begin{aligned}\ln(v_1(s, \rho)) &= s \ln(1 - \rho) + \frac{2 + 2s}{3 + s} \ln \left[ B \left( \frac{1 - s}{4}, 2 \right) \right] \\ &\quad + \frac{1 - s}{3 + s} \ln \left( \frac{1}{a(s)} [2^{a(s)}(1 - \rho)^{-a(s)} - (1 + \rho)^{-a(s)}] \right) \\ &= v_{1,1}(s, \rho) + v_{1,2}(s, \rho),\end{aligned}\tag{4.25}$$

where

$$\begin{aligned}v_{1,1}(s, \rho) &= \frac{1 - s}{3 + s} \ln \left( \frac{1}{a(s)} [2^{a(s)}(1 + \rho)^{a(s)} - (1 - \rho)^{a(s)}] \right) \\ v_{1,2}(s, \rho) &= \left( s - a(s) \frac{1 - s}{3 + s} \right) \ln(1 - \rho) + \frac{2 + 2s}{3 + s} \ln \left[ B \left( \frac{1 - s}{4}, 2 \right) \right] - a(s) \frac{1 - s}{3 + s} \ln(1 + \rho).\end{aligned}\tag{4.26}$$

After careful calculations, we obtain the derivative of  $v_{1,1}(s, \rho)$  with respect to  $s$

$$\begin{aligned}(v_{1,1}(s, \rho))'_s &= - \frac{4}{(s + 3)^2} \ln \left( \frac{2(1 - s)}{s^2 + (4n + 2)s + 4n - 3} \right) \\ &\quad - \frac{4}{(s + 3)^2} \ln [(2 + 2\rho)^{a(s)} - (1 - \rho)^{a(s)}] + \frac{s^2 - 2s - 8n + 1}{(s + 3)(s^2 + (4n + 2)s + 4n - 3)} \\ &\quad + \frac{1 - s}{s + 3} a'(s) \frac{(2 + 2\rho)^{a(s)} \ln(2 + 2\rho) - (1 - \rho)^{a(s)} \ln(1 - \rho)}{(2 + 2\rho)^{a(s)} - (1 - \rho)^{a(s)}} \\ &\geq \frac{4}{(s + 3)^2} \ln \left[ \frac{4n - 3}{2(1 - s)} \right] - \frac{4}{(s + 3)^2} a(s) \ln(2 + 2\rho) \\ &\quad + \frac{s^2 - 2s - 8n + 1}{(s + 3)(s^2 + (4n + 2)s + 4n - 3)} + \frac{-s^2 + 2s + 8n - 1}{2(1 - s)(s + 3)} \ln(2 + 2\rho) \\ &\geq \frac{4}{(s + 3)^2} \ln \left[ \frac{4n - 3}{2(1 - s)} \right] + \left( \frac{1}{2(1 - s)} + \frac{4n}{(s + 3)^2} \right) \ln(2 + 2\rho) \\ &\quad + \frac{s^2 - 2s - 8n + 1}{(s + 3)(s^2 + (4n + 2)s + 4n - 3)} \\ &\geq \frac{1}{4} \ln \left( \frac{12n - 9}{4} \right) + \left( \frac{1}{2} + \frac{n}{4} \right) \ln 2 - \frac{72}{160} - \frac{26}{160n - \frac{200}{3}} \geq 0,\end{aligned}\tag{4.27}$$

since  $\frac{s^2 - 2s - 8n + 1}{(s + 3)(s^2 + (4n + 2)s + 4n - 3)}$  is an increasing function. Thus  $v_{1,1}(s, \rho)$  is increasing with respect to  $s$ . For  $v_{1,2}(s, \rho)$ , we have

$$\begin{aligned}v_{1,2}(s, \rho) &= \left( s - a(s) \frac{1 - s}{3 + s} \right) \ln(1 - \rho) + \frac{2 + 2s}{3 + s} \left( \ln \Gamma(n) + \ln \prod_{k=0}^{n-1} \frac{1}{1 - s + 4k} \right) \\ &\quad + \left( \frac{2 + 2s}{3 + s} \ln(4^n) - a(s) \frac{1 - s}{s + 3} \ln(1 + \rho) \right) \\ &:= A_1 + A_2 + A_3.\end{aligned}\tag{4.28}$$

It is easily to obtain  $A_1$  and  $A_2$  are increasing with respect to  $s$ . We find

$$A_3 = \left[ \frac{8ns + 8n}{s + 3} - a(s) \frac{1 - s}{s + 3} \right] \ln 2 + a(s) \frac{1 - s}{s + 3} [\ln 2 - \ln(1 + \rho)] \quad (4.29)$$

Since  $\left[ \frac{8ns + 8n}{2(s+3)} - a(s) \frac{1-s}{s+3} \right]' = \frac{-s^2 - 6s - 9 + 8n}{2(s+3)^2} \geq 0$  and  $[a(s) \frac{1-s}{s+3}]' = \frac{s^2 + 6s + 8n + 9}{2(s+3)^2} > 0$ ,  $A_3$  is increasing with respect to  $s$ . Combining the monotonicity of  $v_1(s, \rho)$  and  $\max\{C_5(n, s), C_6(n, s)\}$  with respect to  $s$ ,  $v(s, \rho)$  will when  $s$  grows for  $s > \frac{1}{3}$ . Similarly, we can derive the same result for  $s \leq \frac{1}{3}$ . Thus we obtain the desired result.  $\square$

When  $s \rightarrow 1$ , the upper bounds for the expected stopping steps can not work, since fractional Laplacian degenerates into the classical Laplace operator so that the Lévy flight becomes Brownian motion. Though the Brownian motion originated at  $x$  will reach boundary  $\mathbb{B}_r$  in the probability sense, the expected stopping steps are infinite. We also have the following theorem.

**Theorem 4.2.** *When  $s \rightarrow 1$ ,  $G(x, y)$  in (2.4) is the Green function for the classical Laplace equation with ball boundary.*

*Proof.* When  $n = 2$ , we have

$$\begin{aligned} G(x, y) &= \kappa(2, 1) \int_0^{r^*(x, y)} \frac{1}{1+t} dt = \kappa(2, 1) \log \left( \frac{(r^2 - |x|^2)(r^2 - |y|^2) + r^2|x-y|^2}{r^2|x-y|^2} \right) \\ &= \frac{1}{4\pi} \log \left( \frac{r^4 + |x|^2|y|^2 - 2r^2|x||y| \cos \langle x, y \rangle}{r^2|x-y|^2} \right). \end{aligned} \quad (4.30)$$

When  $n \geq 3$ , we have

$$\begin{aligned} G(x, y) &= \kappa(n, 1) |x-y|^{2-n} \int_0^{r^*(x, y)} \frac{1}{(1+t)^{\frac{n}{2}}} dt \\ &= \frac{2\kappa(n, 1)}{n-2} |x-y|^{2-n} \left[ 1 - \left( \frac{(r^2 - |x|^2)(r^2 - |y|^2)}{r^2|x-y|^2} + 1 \right)^{-\frac{n-2}{2}} \right] \\ &= \frac{2\kappa(n, 1)}{n-2} \left[ \frac{1}{(|x|^2 + |y|^2 - 2|x||y| \cos \langle x, y \rangle)^{\frac{n-2}{2}}} - \frac{r^{n-2}}{(r^4 + |x|^2|y|^2) - 2r^2 \cos \langle x, y \rangle^{\frac{n-2}{2}}} \right] \end{aligned} \quad (4.31)$$

$\square$

**Remark 4.1.** *When  $f(x) = (d(x))^{-2s}$  which doesn't satisfy the condition in Theorem 2.1, we know that  $u(x)$  in (4.9) is still the solution of the problem (4.2) in the sense of mild solution, while  $u(x)$  may not satisfy the regularity in Theorem 2.1.*

## 5. Numerical examples

In this section, numerical examples are carried out by using Scheme I (quadrature method 2.26 and 2.31) discussed in Section 2 and Algorithm 3.2 introduced in Section 3 on an i5-8250U CPU.

In the experiments, we consider two special cases of equation (1.1): the homogeneous equation with inhomogeneous boundary value condition, and nonconstant source term with homogeneous boundary value condition.

We set step sizes  $h = h_\rho = h_\theta = h_t = h_r$ ,  $r = 1, 2, \dots, n-2$ . In addition,  $E(h) = |u_{2h} - u_h|$  denotes posteriori error estimates in Scheme I and  $E$  denotes the absolute error in the modified walk-on-sphere method. Then the convergence order is given by  $rate = \log_2 \frac{E(2h)}{E(h)}$ .

**Example 5.1.** Let  $\Omega$  be a unit ball in  $\mathbb{R}^n$  centered at the origin

$$\begin{cases} (-\Delta)^s u(\mathbf{x}) = 0, & \mathbf{x} \in \Omega, \\ u(\mathbf{x}) = g(\mathbf{x}), & \mathbf{x} \in \mathbb{R}^n \setminus \Omega, \end{cases} \quad (5.1)$$

where  $g(\mathbf{x}) = \exp(-|\mathbf{x} - \mathbf{x}'|^2)$ .

In this example, we take  $s = 0.25, 0.5, 0.75$  and set different step sizes  $\frac{1}{32}, \frac{1}{64}, \frac{1}{128}, \frac{1}{256}, \frac{1}{512}$  in two spacial dimensions and  $\frac{1}{8}, \frac{1}{16}, \frac{1}{32}, \frac{1}{64}, \frac{1}{128}$  in three spacial dimensions for Scheme I. For the modified walk-on-sphere method, the number of samples are set by 1000, 10000, 100000. We evaluate  $u(0.6, 0.6)$  with  $\mathbf{x}' = (3, 0)$  in two spacial dimensions. The numerical results of Scheme I and modified walk-on-sphere method are presented in Tables 1 and 2, respectively.

Table 1: Numerical results of Example 5.1 using Scheme I in 2D.

$s$	$\frac{1}{h}$	approximation	$E(h)$	rate	CPU time(secs.)
$s = 0.25$	32	0.0234077	5.6370E-06	—	0.0631
	64	0.0234021	8.9306E-07	2.6581	0.1039
	128	0.0234012	2.2166E-07	2.0104	0.3229
	256	0.0234009	5.5441E-08	1.9994	1.1362
	512	0.0234009	1.3863E-08	1.9996	4.4059
$s = 0.50$	32	0.0187671	8.2695E-06	—	0.0595
	64	0.0187558	4.6391E-07	4.1559	0.1041
	128	0.0187583	1.1117E-07	2.0612	0.3031
	256	0.0187582	2.8056E-08	1.9863	1.0778
	512	0.0187582	7.0603E-09	1.9905	4.1187
$s = 0.75$	32	0.0099238	1.5558E-05	—	0.0599
	64	0.0099082	3.7635E-07	5.3694	0.1407
	128	0.0099079	8.3237E-08	2.1768	0.7417
	256	0.0099078	2.1912E-08	1.9255	1.4891
	512	0.0099077	5.7075E-09	1.9407	5.5057

Table 1 shows the convergent order coincides with the theoretical analysis. It can be seen from Table 2 that the simulation results by the Monte Carlo method are close to the approximations in Table 1.

Next, we evaluate  $u(0.5, 0.5, 0.5)$  with  $\mathbf{x}' = (3, 0, 0)$  in three spacial dimensions. Numerical results are given in Tables 3 and 4. Table 3 shows that although Scheme I achieves same

Table 2: Numerical results of Example 5.1 using modified walk-on-sphere method in 2D.

$s$	samples	approxiamtion	average no. steps	variance	CPU time(secs.)
$s = 0.25$	1000	0.0230409	1.7470	9.4958E-03	0.0078
	10000	0.0231043	1.7515	9.0476E-03	0.0835
	100000	0.0234345	1.7543	8.4807E-03	0.6804
$s = 0.50$	1000	0.0185969	2.9460	1.0672E-02	0.0171
	10000	0.0188054	3.0495	5.8763E-03	0.1179
	100000	0.0187276	3.0142	5.7382E-03	1.1908
$s = 0.75$	1000	0.0098083	6.4760	3.2685E-03	0.0295
	10000	0.0097991	6.2111	2.1455E-03	0.2601
	100000	0.0098974	6.1990	1.7594E-03	2.5103

convergent order while the CPU time in three spacial dimensions grows a lot. Compared with the Scheme I, modified walk-on-sphere method presented in Table 4 saves much more time.

Table 3: Numerical results of Example 5.1 using Scheme I in 3D.

$s$	$\frac{1}{h}$	approximation	$E(h)$	rate	CPU time(secs.)
$s = 0.25$	8	0.0084161	7.3967E-05	—	0.0983
	16	0.0079807	9.5757E-05	3.4423	0.2698
	32	0.0080208	2.1302E-05	2.1448	1.3501
	64	0.0080298	4.9834E-06	2.0779	14.830
	128	0.0080320	1.2291E-06	2.0155	103.99
$s = 0.50$	8	0.0066376	7.3967E-05	—	0.0752
	16	0.0065636	9.5757E-06	-0.3725	0.2861
	32	0.0066594	2.1377E-05	2.1684	1.2785
	64	0.0066807	4.6231E-06	2.0957	9.4483
	128	0.0066856	1.0635E-06	2.0195	78.617
$s = 0.75$	8	0.0033824	2.7559E-04	—	0.0792
	16	0.0036580	1.5625E-04	0.8185	0.2571
	32	0.0038143	3.4898E-05	2.1627	1.3584
	64	0.0038491	8.0415E-06	2.1176	10.167
	128	0.0038572	1.9762E-06	2.0247	85.237

**Example 5.2.** Consider equation (5.1) with  $\Omega$  being a unit ball in  $\mathbb{R}^n$  centered at the origin,

$$g(x) = \begin{cases} \frac{1}{\pi} \log |x - x'|, & n = 1, \\ a(n, s) |x - x'|^{-n+2s}, & n \geq 2, \end{cases} \quad (5.2)$$

and

$$a(n, s) = \frac{\Gamma(\frac{n}{2} - s)}{2^{2s} \pi^{\frac{n}{2}} \Gamma(s)}. \quad (5.3)$$

Table 4: Numerical results of Example 5.1 for modified walk-on-sphere method in 3D.

$s$	samples	approximation	average no. steps	variance	CPU time(secs.)
$s = 0.25$	1000	0.0083326	1.8890	2.2310E-03	0.0340
	10000	0.0080532	1.9248	1.9605E-03	0.1520
	100000	0.0080475	1.9259	1.8473E-03	1.3697
$s = 0.50$	1000	0.0068445	3.9280	3.1425E-03	0.0476
	10000	0.0067445	3.8514	1.3806E-03	0.3632
	100000	0.0066647	3.8748	1.2729E-03	2.7069
$s = 0.75$	1000	0.0039063	10.327	1.8671E-03	0.0936
	10000	0.0037649	10.010	5.4232E-04	0.7213
	100000	0.0038088	10.110	4.1431E-04	7.4822

Here  $g(x)$  is just Green's function and  $x' \in \mathbb{R}^n \setminus \Omega$ , where  $x'$  can be any points out of the unit ball. The exact solution to (5.1) is given below [7],

$$u(x) = \begin{cases} \frac{1}{\pi} \log |x - x'|, & n = 1, \\ a(n, s) |x - x'|^{-n+2s}, & n \geq 2. \end{cases} \quad (5.4)$$

We use the modified walk-on-sphere method to simulate the solution. The number of samples are set by 1000, 10000, and 100000 for modified walk-on-sphere method. Though  $g(x)$  does not satisfy the condition in Theorem 2.1, modified walk-on-sphere method still takes effect since the representation formula is finite. The value of  $u(\frac{1}{2})$  with  $x' = 2$  in one spacial dimension is showed in Table 5. We also evaluate  $u(0.6, 0.6)$  with  $x' = (\sqrt{2}, \sqrt{2})$  in two spacial dimensions. Table 6 gives the numerical results. The average number of step in Table 6 is basically the same as that in Table 2, indicating that the average number of step isn't related to  $g(x)$ . When  $10^5$  samples are used in modified walk-on-sphere method, Figure 6 shows that the larger the  $s$  is, the smaller the errors will be, which is caused by the singularity of  $g(x)$ . And the average number of steps will increase when  $s$  tends to 1, which explains why the CPU time will become longer when  $s$  grows.

Table 5: Numerical results of Example 5.2 using modified walk-on-sphere method method in 1D.

$s$	samples	$E$	average no. steps	variance	CPU time(secs.)
$s = 0.25$	1000	8.8457E-03	1.2910	3.1650E-01	0.0129
	10000	2.2407E-03	1.2929	2.4775E-01	0.0912
	100000	8.4281E-04	1.2915	2.3637E-01	0.8159
$s = 0.50$	1000	6.9838E-03	1.5000	2.8124E-01	0.0150
	10000	3.7475E-03	1.5290	2.7348E-01	0.0982
	100000	4.8992E-04	1.5246	2.6451E-01	0.8901
$s = 0.75$	1000	7.8929E-03	1.7200	3.7211E-01	0.0253
	10000	3.1675E-03	1.7069	3.7141E-01	0.1236
	100000	2.8304E-05	1.6879	3.5764E-01	1.1568

Table 6: Numerical results of Example 5.2 using modified walk-on-sphere method in 2D.

$s$	samples	$E$	average no. steps	variance	CPU time(secs.)
$s = 0.25$	1000	7.7764E-03	1.7220	1.5125E-01	0.0191
	10000	3.3265E-03	1.7338	3.3816E-02	0.1893
	100000	1.7565E-03	1.7338	1.2221E-02	1.6108
$s = 0.50$	1000	2.3412E-03	3.0770	1.4768E-02	0.0292
	10000	1.3937E-04	3.0016	8.2579E-03	0.2636
	100000	7.8162E-05	3.0004	6.7842E-03	2.5823
$s = 0.75$	1000	9.5021E-03	6.5530	4.0156E-02	0.0813
	10000	1.0741E-04	6.2859	3.6001E-02	0.5657
	100000	2.2905E-05	6.2344	2.9957E-02	5.5934

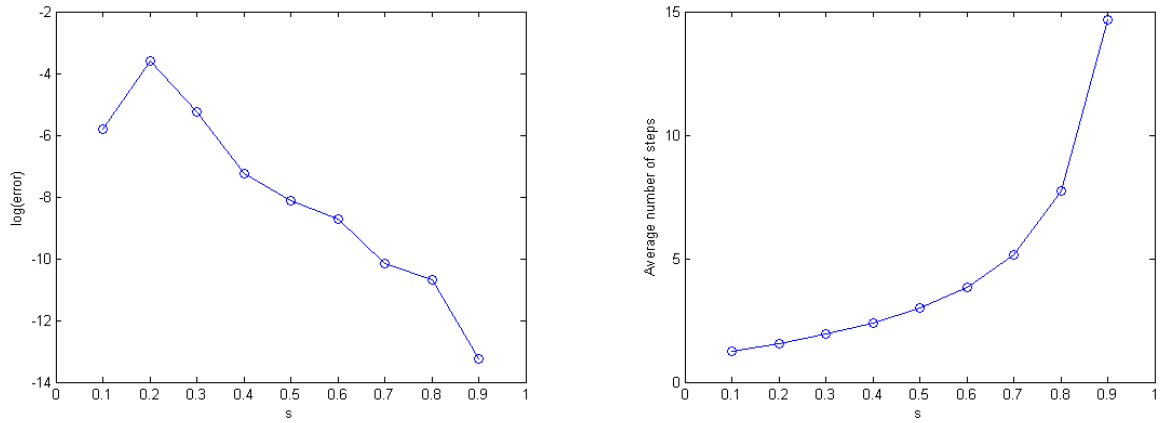


Figure 6: Result for Example 5.1 with the walk-one-spheres method based on  $10^5$  samples in two dimensions. When  $s$  becomes bigger, the error will be smaller whereas the average number of steps will increase.



Next, we evaluate  $u(0.5, 0.5, 0.5)$  with  $\mathbf{x}' = (\frac{2\sqrt{3}}{3}, \frac{2\sqrt{3}}{3}, \frac{2\sqrt{3}}{3})$  in three spacial dimensions. The numerical results are given in Table 7. The consuming time does not grow too much as the dimension increases. Figure 7 also indicates the relation between the average number of step and index  $s$  remains, which coincides with theoretical analysis.

Table 7: Numerical results of Example 5.2 for modified walk-on-sphere method in 3D.

$s$	samples	$E$	average no. steps	variance	CPU time(secs.)
$s = 0.25$	1000	5.0191E-03	1.8500	1.7617E-04	0.0213
	10000	9.5331E-04	1.9544	1.2973E-04	0.1645
	100000	3.9997E-04	1.9544	3.5799E-05	1.5001
$s = 0.50$	1000	2.1632E-03	4.0730	8.7991E-05	0.0318
	10000	6.4897E-04	3.8937	5.2222E-05	0.2899
	100000	2.4870E-05	3.8930	2.2081E-05	2.7808
$s = 0.75$	1000	3.1106E-03	9.8970	3.3897E-05	0.1346
	10000	5.4258E-05	10.181	2.6497E-05	0.8003
	100000	3.6118E-05	10.200	2.0900E-05	7.4063

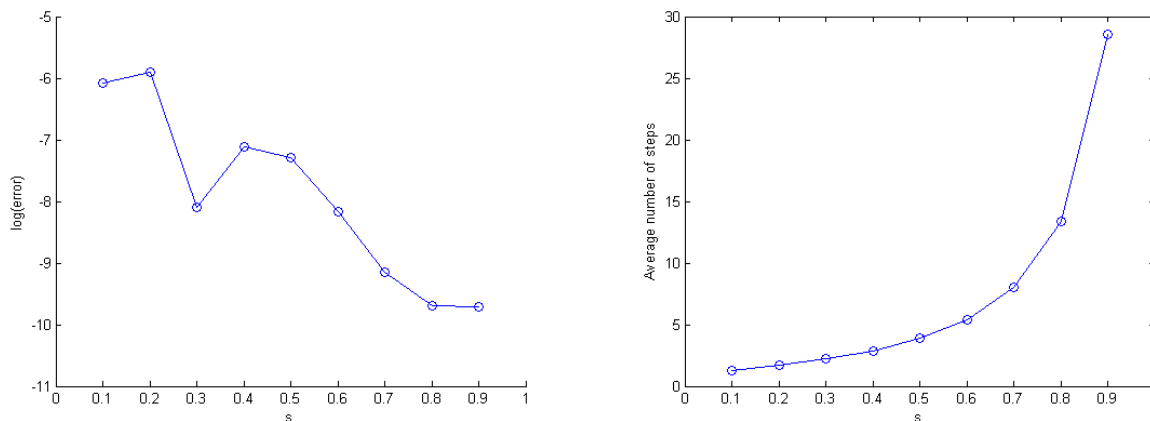


Figure 7: Result for Example 5.1 with the walk-one-spheres method based on  $10^5$  samples in three dimensions. The error and average number of steps keep the same tendency as those in 2D when  $s$  tends to 1 from 0.

For higher dimensional cases, we first evaluate  $u(\mathbf{x})$  with  $\mathbf{x} = \frac{1}{4} * \mathbf{ones}(4)$  and  $\mathbf{x}' = \mathbf{ones}(4)$  in four spacial dimensions and  $u(\mathbf{x})$  with  $\mathbf{x} = \frac{1}{5} * \mathbf{ones}(5)$  and  $\mathbf{x}' = \frac{2\sqrt{5}}{5} * \mathbf{ones}(5)$  in five spacial dimensions, where  $\mathbf{ones}(n)$  is an  $n$ -dimensional vector with all ones. The number of samples are set by  $10^5$ . Since when  $s \in (0, \frac{1}{2})$ ,  $g(x)$  has singularity, we mainly give the numerical results for  $s \in (\frac{1}{2}, 1)$  in Table 8.

We then evaluate  $u(\mathbf{x})$  with  $\mathbf{x} = \frac{1}{10} * \mathbf{ones}(10)$  and  $\mathbf{x}' = \frac{\sqrt{10}}{5} * \mathbf{ones}(10)$  in ten spacial dimensions. The number of samples are set by  $10^5$  and the numerical results is given in Table 9. Compared with the computational time in lower dimensions, the time in ten dimensions only increases in multiple, which shows the efficiency of the algorithm.

Table 8: Numerical results of Example 5.2 for modified walk-on-sphere method in 4D and 5D by  $10^5$  samples.

$s$	$n$	$E$	average no. steps	variance	CPU time(secs.)
$s = 0.25$	$n = 4$	1.1203E-02	1.5387	2.1507E-01	5.8991
$s = 0.50$	$n = 4$	2.0822E-03	3.3463	8.8047E-02	12.082
$s = 0.60$	$n = 4$	1.4179E-03	5.0610	4.8773E-02	19.741
$s = 0.70$	$n = 4$	6.4099E-04	8.2784	1.9234E-02	32.903
$s = 0.80$	$n = 4$	3.4514E-04	15.663	8.9541E-03	60.322
$s = 0.90$	$n = 4$	2.8155E-04	38.629	2.9072E-03	208.21
$s = 0.25$	$n = 5$	1.7871E-03	1.5178	4.6222E-02	8.7034
$s = 0.50$	$n = 5$	1.6622E-03	3.4818	2.8613E-02	19.241
$s = 0.60$	$n = 5$	8.2384E-04	5.4826	1.6533E-02	30.330
$s = 0.70$	$n = 5$	6.3443E-04	9.4176	8.4255E-03	52.100
$s = 0.80$	$n = 5$	3.4322E-04	18.598	2.2152E-03	100.84
$s = 0.90$	$n = 5$	2.9972E-04	48.296	1.0710E-03	271.01

Table 9: Numerical results of Example 5.2 for modified walk-on-sphere method in 10D by  $10^5$  samples.

$s$	$n$	$E$	average no. steps	variance	CPU time(secs.)
$s = 0.25$	$n = 10$	1.1617E-03	1.4501	2.4291E-01	23.991
$s = 0.50$	$n = 10$	6.8564E-04	3.6944	7.5413E-02	52.489
$s = 0.60$	$n = 10$	5.3812E-04	6.4110	5.2138E-04	94.023
$s = 0.70$	$n = 10$	2.9153E-04	12.266	2.4223E-04	178.82
$s = 0.80$	$n = 10$	2.4108E-04	27.366	6.1517E-05	395.73
$s = 0.90$	$n = 10$	1.2341E-04	80.842	5.4785E-05	1168.0

**Example 5.3.** Consider the following fractional Poisson equation with vanishing Dirichlet boundary condition

$$\begin{cases} (-\Delta)^s u(\mathbf{x}) = f(\mathbf{x}), & \mathbf{x} \in \Omega, \\ u(\mathbf{x}) = 0, & \mathbf{x} \in \mathbb{R}^n \setminus \Omega, \end{cases} \quad (5.5)$$

where  $\Omega$  is a unit ball in  $\mathbb{R}^n$  and

$$f(\mathbf{x}) = \begin{cases} \Gamma\left(\frac{s}{2} + 2\right) x, & n = 1, \\ 2^{2s} \Gamma(2 + s) \Gamma\left(\frac{n}{2} + s\right) \Gamma\left(\frac{n}{2}\right)^{-1} \left(1 - \left(1 + \frac{2s}{n}\right) |\mathbf{x}|^2\right), & n \geq 2. \end{cases} \quad (5.6)$$

The exact solution to (5.8) is given in [16]

$$u(\mathbf{x}) = \begin{cases} x(1 - x^2)^s, & n = 1, \\ (1 - |\mathbf{x}|^2)^{1+s}, & n \geq 2. \end{cases} \quad (5.7)$$

We use the modified walk-on-sphere method to simulate the solution and the number of samples are set by 1000, 10000, and 100000 for modified walk-on-sphere method. We evaluated  $u(\frac{1}{2})$  in one spacial dimension, which is showed in Table 10. Since we need to approximate the integral or the hypergeometric function when  $\frac{1}{2} < s < 1$ , the computational time is a bit longer.  $u(0.6, 0.6)$  is also evaluated in two spacial dimensions by both Scheme I (2.31) and the modified walk-on-sphere method. The numerical results are presented in Tables 11 and 12. It is obvious that Scheme I has bigger errors and costs more computational time. Comparing Table 2 and Table 6, it is obvious that the average number of step is independent of  $f(\mathbf{x})$  and  $g(\mathbf{x})$ . Figure 8 shows that there is no obvious trend in absolute error when  $s$  changes. As expected, we again observe that when  $\mathbf{x}$  is closed to the origin, the average number of steps will become smaller. In particular, when  $\mathbf{x}$  is at the origin, the number of steps is one.

Table 10: Numerical results of Example 5.3 using modified walk-on-sphere method in 1D.

$s$	samples	$E$	average no. steps	variance	CPU time(secs.)
$s = 0.25$	1000	9.9759E-03	1.2540	1.1209E-01	0.0159
	10000	8.7500E-04	1.2952	1.1191E-01	0.1131
	100000	4.6390E-04	1.2879	1.0927E-01	0.8675
$s = 0.50$	1000	9.4393E-03	1.5410	1.7148E-01	0.0178
	10000	2.9952E-03	1.5316	1.6840E-01	0.1139
	100000	2.0324E-04	1.5281	1.6630E-01	0.9490
$s = 0.75$	1000	3.5671E-03	1.7000	8.6924E-01	0.8696
	10000	1.6581E-03	1.6945	2.3160E-01	6.3171
	100000	4.2174E-04	1.6838	2.7423E-01	45.534

Next, we evaluate  $u(0.5, 0.5, 0.5)$  in three spacial dimensions. Table 13 shows that the CPU time of modified walk-on-sphere method does not increase too much in three dimensions

Table 11: Numerical results of Example 5.3 for modified walk-on-sphere method in 2D.

$s$	samples	$E$	average no. steps	variance	CPU time(secs.)
$s = 0.25$	1000	6.9086E-03	1.7620	1.1539E-01	0.0216
	10000	3.1608E-03	1.7716	1.0973E-01	0.1662
	100000	1.3496E-04	1.7606	8.7965E-02	1.5673
$s = 0.50$	1000	6.4914E-03	2.8210	1.9263E-01	0.0332
	10000	2.6209E-03	2.9709	1.7505E-01	0.2636
	100000	1.3063E-04	2.9997	1.7088E-01	2.8465
$s = 0.75$	1000	9.5021E-03	5.9050	2.2955E-01	0.0538
	10000	1.0741E-04	6.1569	2.1898E-01	0.5109
	100000	2.2905E-05	6.1818	1.8771E-01	5.6996

Table 12: Numerical results of Example 5.1 using Scheme I (2.31) in 2D.

$s$	$\frac{1}{h}$	$E(h)$	rate	CPU time(secs.)
$s = 0.25$	32	3.4047E-02	—	0.9227
	64	2.5291E-02	0.5159	10.797
	128	1.9142E-02	0.5099	53.474
	256	1.4927E-02	0.5462	246.99
	512	1.2011E-02	0.5317	1922.1
$s = 0.50$	32	8.6860E-03	—	0.6604
	64	4.7663E-03	0.4627	4.2421
	128	2.7036E-03	0.9262	36.764
	256	1.6377E-03	0.9524	335.90
	512	1.0602E-03	0.8392	1712.6
$s = 0.75$	32	1.1589E-02	—	0.7423
	64	4.6710E-03	0.9681	5.3990
	128	1.8928E-03	1.3157	39.301
	256	8.2243E-04	1.3769	441.43
	512	3.9633E-04	1.3286	2169.6

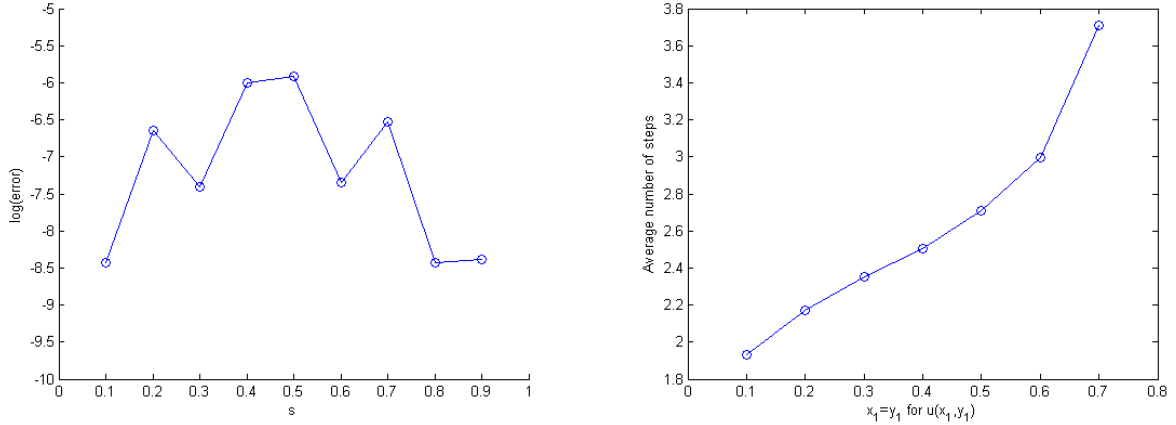


Figure 8: Result for Example 5.2 with the walk-one-sphere method based on  $10^5$  samples in two dimensions. From the left to right, we see there is no obvious relation between errors and  $s$ , meanwhile, when  $x$  is near the origin, the average number of steps will be small.

compared with the time in two dimensions. Figure 9 gives the same result derived in Figure 8. When  $x$  approaches the origin, the average number of steps will be small, which coincides with the theoretical analysis.

Table 13: Numerical results of Example 5.3 for modified walk-on-sphere method in 3D.

$s$	samples	$E$	average no. steps	variance	CPU time(secs.)
$s = 0.25$	1000	4.2582E-03	1.8890	7.4618E-02	0.0327
	10000	8.6731E-04	1.9480	7.2944E-02	0.1464
	100000	1.5456E-04	1.9233	7.2383E-02	1.4511
$s = 0.50$	1000	7.2182E-03	3.9970	1.1093E-01	0.0348
	10000	1.7504E-04	3.8960	1.0408E-01	0.3011
	100000	1.3108E-04	3.9187	1.0043E-01	2.9787
$s = 0.75$	1000	9.3257E-04	10.357	1.2448E-01	0.0810
	10000	5.2534E-04	10.067	1.1665E-01	0.7787
	100000	2.5671E-04	10.132	1.1586E-01	7.7002

For higher dimensional cases, we still first evaluate  $u(x)$  with  $x = \frac{1}{4} * \mathbf{ones}(4)$  in four spacial dimensions and  $u(x)$  with  $x = \frac{1}{5} * \mathbf{ones}(5)$  in five spacial dimensions. The number of samples are set by  $10^5$  and the numerical results is given in Table 14. It is noticed that the average number of steps will increase when the fractional order  $s$  increases.

We then evaluate  $u(x)$  with  $x = \frac{1}{10} * \mathbf{ones}(10)$  in ten spacial dimensions. The number of samples are set by  $10^5$ . Unlike the homogeneous equation in Examples 5.1 and 5.2, we need to sample  $Y$  in every step so that it will cost more computational time. However, based on the numerical results given in Table 15 the algorithm is still fast and efficient.

Next, we gives the experiment of fractional Poisson equation with square boundary.

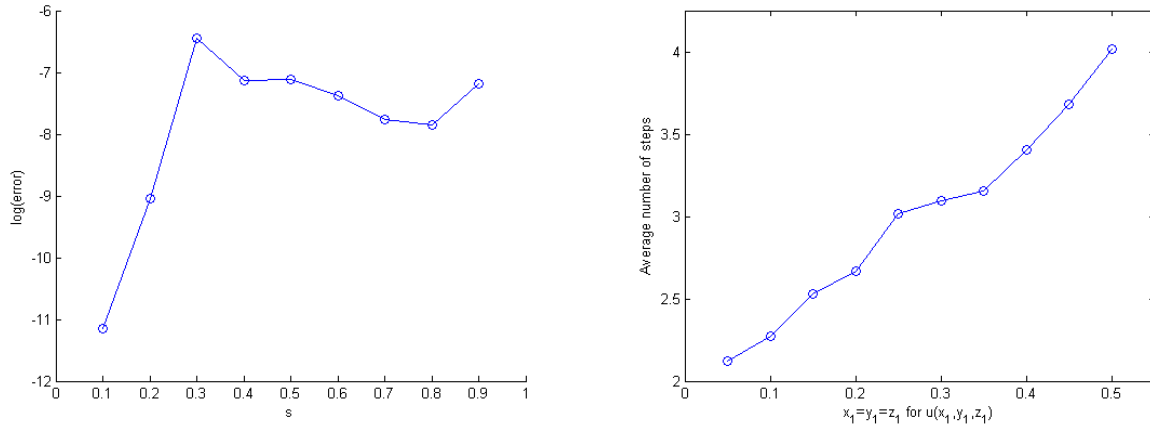


Figure 9: Result for Example 5.2 with the walk-one-sphere method based on  $10^5$  samples in three dimensions. From the left to right, we derive the same results as those in two dimensions.

Table 14: Numerical results of Example 5.3 for modified walk-on-sphere method in 4D and 5D by  $10^5$  samples.

$s$	$n$	$E$	average no. steps	variance	CPU time(secs.)
$s = 0.20$	$n = 4$	1.0203E-03	1.3759	7.0657E-02	10.931
$s = 0.40$	$n = 4$	3.8298E-04	2.3480	1.3780E-01	18.279
$s = 0.60$	$n = 4$	5.9519E-04	5.0809	1.9744E-01	40.125
$s = 0.80$	$n = 4$	6.2239E-04	15.702	2.5873E-01	121.50
$s = 0.20$	$n = 5$	9.3904E-04	1.3557	5.8018E-02	16.349
$s = 0.40$	$n = 5$	5.6123E-04	2.3758	1.1718E-01	28.644
$s = 0.60$	$n = 5$	9.7228E-04	5.4498	1.6952E-01	65.567
$s = 0.80$	$n = 5$	2.5286E-03	18.684	2.2059E-01	221.95

Table 15: Numerical results of Example 5.3 for modified walk-on-sphere method in 10D by  $10^5$  samples.

$s$	$n$	$E$	average no. steps	variance	CPU time(secs.)
$s = 0.10$	$n = 10$	2.1003E-04	1.0953	1.9213E-02	34.905
$s = 0.30$	$n = 10$	1.6807E-03	1.6611	5.9872E-02	49.659
$s = 0.50$	$n = 10$	6.3033E-03	3.6920	9.9123E-02	110.85
$s = 0.70$	$n = 10$	2.8531E-03	12.230	1.3642E-01	344.63
$s = 0.90$	$n = 10$	1.8440E-03	80.954	1.6415E-01	2955.7

**Example 5.4.** Consider the following fractional Poisson equation with vanishing Dirichlet boundary condition

$$\begin{cases} (-\Delta)^s u(\mathbf{x}) = f(\mathbf{x}), & \mathbf{x} \in [0, 1]^n, \\ u(\mathbf{x}) = 0, & \mathbf{x} \in \mathbb{R}^n \setminus [0, 1]^n, \end{cases} \quad (5.8)$$

where  $f(x) = 1$ .

We evaluate  $u(\mathbf{x})$  at points  $\mathbf{x}_1 = \frac{1}{1000} * \mathbf{ones}(10)$  and  $\mathbf{x}_2 = \frac{1}{10} * \mathbf{ones}(10)$  in ten spacial dimensions, respectively. The number of samples are set by  $10^5$ . It is reasonable that numerical results are closed to the exact solution, since when  $\mathbf{x}$  is near boundary, numerical solutions are almost equal to 0. Average number of steps will increase, when  $s$  grows, while it seems no relations between average number of steps and location  $\mathbf{x}$ .

Table 16: Numerical results of Example 5.4 for modified walk-on-sphere method in 10D.

location	$s$	approximation	average no. steps	variance	CPU time(secs.)
$\mathbf{x}_1$	0.25	7.711E-03	1.9009	1.9791E-05	61.980
	0.50	5.244E-05	5.7405	1.3905E-09	125.64
	0.75	3.227E-07	26.661	6.0199E-14	409.68
$\mathbf{x}_2$	0.25	2.430E-01	1.8899	1.9093E-02	62.886
	0.50	5.250E-02	5.7755	1.3489E-03	120.84
	0.75	1.023E-02	26.781	6.0105E-05	409.18

**Remark 5.1.** Since the numerical experiments for modified walk-on-sphere method contain randomness, the variance sometimes does not converge (e.g. Table 15).

As discussed in Section 4, the average number of steps depends only on the domain  $\Omega$ , the point  $\mathbf{x}$  at which the solution we want to arrive, and  $s$ . Combining Figures 6-9, we conclude that when  $\Omega$  is a ball, the steps will increase if  $\mathbf{x}$  is far from the center of the sphere or  $s$  becomes larger.

## 6. Conclusion

We propose a modified walk-on-sphere method for the fractional Laplacian problem on general domains in high dimensions. Based on the probabilistic representation of the problem, we carefully compute the probabilities of the random walks, using proper quadrature rules and the modified walk-on-sphere method to sample from the probabilities. We show that the quadrature rules are of second-order convergent when the boundary data  $g(\mathbf{x}) \in C_b^2(\mathbb{R}^n \setminus \mathbb{B}_r)$  and the forcing  $f = 0$ . When  $f(\mathbf{x}) \in C_b^2(\mathbb{B}_r \setminus S_h)$  and  $g(\mathbf{x}) = 0$ , we derive the numerical method in two dimensions, while the convergent order is only  $\mathcal{O}(h^{2s \wedge 1})$  because of the poor property of Green function and it will cost more computational time. So, it is necessary to propose much more efficient method for the problem. Thus, for problems in higher dimensions, we apply an efficient rejection sampling method based on truncated Gaussian distribution. Also, we estimate the mean of the number of walks for the problem

in a ball in  $n$  ( $n \geq 2$ ) dimensions and  $s \in (0, 1)$  and show that the mean of the number of walks is increasing in  $s$  and the distance of the initial point to the origin. Numerical results verify the theoretical analysis and show the efficiency of the proposed method. Extensions to fractional advection-diffusion equations are currently ongoing.

## References

- [1] G. Acosta and J. P. Borthagaray, A fractional Laplace equation: regularity of solutions and finite element approximations, *SIAM J. Numer. Anal.*, 55 (2017), pp. 472–495.
- [2] G. Acosta, J. P. Borthagaray, O. Bruno, and M. Maas, Regularity theory and high order numerical methods for the (1D)-fractional Laplacian, *Math. Comput.*, 87 (2018), pp. 1821–1857.
- [3] R. A. Adams, *Sobolev Spaces*, Academic Press, New York, 1975.
- [4] M. Ainsworth and C. Glusa, Towards an efficient finite element method for the integral fractional Laplacian on polygonal domains, in *Contemporary computational mathematics—a celebration of the 80th birthday of Ian Sloan*, Springer, Cham, 2018, pp. 17–57.
- [5] D. Applebaum, *Lévy Processes and Stochastic Calculus*, Cambridge University Press, Cambridge, UK, 2009.
- [6] A. Bonito, J. P. Borthagaray, R. H. Nochetto, E. Otárola, and A. J. Salgado, Numerical methods for fractional diffusion, *Comput. Vis. Sci.*, 19 (2018), pp. 19–46.
- [7] C. Bucur, Some observations on the Green function for the ball in the fractional Laplace framework, *Commun. Pure Appl. Anal.*, 15(2) (2016), pp. 657–699.
- [8] M. Cai and C. P. Li, On Riesz derivative, *Fract. Calc. Appl. Anal.*, 22(2) (2019), pp. 287–301.
- [9] Z. Q. Chen and R. M. Song, Estimates on Green functions and Poisson kernels for symmetric stable processes, *Math. Ann.*, 312(3) (1998), pp. 465–501.
- [10] N. Chopin, Fast simulation of truncated Gaussian distributions, *Stat. Comput.*, 21(2) (2011), pp. 275–288.
- [11] S. Das, *Functional Fractional Calculus*, Springer-Verlag, Berlin, 2011.
- [12] J. M. Delaurentis and L. A. Romero, A Monte Carlo method for Poisson’s equation, *J. Comput. Phys.*, 90 (1990), pp. 123–140.
- [13] M. D’Elia, Q. Du, C. Glusa, M. Gunzburger, X. Tian, and Z. Zhou, Numerical methods for nonlocal and fractional models, *Acta Numerica*, (2021).
- [14] M. D’Elia and M. Gunzburger, The fractional Laplacian operator on bounded domains as a special case of the nonlocal diffusion operator, *Comput. Math. Appl.*, 66 (2013), pp. 1245–1260.
- [15] S. W. Duo, H. W. Van Wyk, and Y. Z. Zhang, A novel and accurate finite difference method for the fractional Laplacian and the fractional Poisson problem, *J. Comput. Phys.*, 355 (2018), pp. 233–252.
- [16] B. Dyda, Fractional calculus for power functions and eigenvalues of the fractional Laplacian, *Fract. Calc. Appl. Anal.*, 15(4) (2012), pp. 536–555.
- [17] B. S. Elepov and G. A. Mihailov, The ‘walk on spheres’ algorithm for the equation  $\delta u - cu = -g$ , *Sov. Math. Dokl.*, 14 (1973), pp. 1276–1280.
- [18] T. Gao, J. Q. Duan, X. F. Li, and R. M. Song, Mean exit time and escape probability for dynamical systems driven by Lévy noises, *SIAM J. Sci. Comput.*, 36(3) (2014), pp. A887–A906.
- [19] Z. Hao and Z. Zhang, Optimal regularity and error estimates of a spectral Galerkin method for fractional advection-diffusion-reaction equation, *SIAM J. Numer. Anal.*, 58(1) (2020), pp. 211–233.
- [20] R. Herrmann, *Fractional Calculus: An Introduction for Physicists*, World Scientific, Singapore, 2011.
- [21] R. Hilfer, *Applications of Fractional Calculus in Physics*, World Scientific, River Edge, NJ, 2000.



- [22] Y. H. Huang and A. Oberman, Numerical methods for the fractional Laplacian: a finite difference-quadrature approach, *SIAM J. Numer. Anal.*, 52(6) (2014), pp. 3056–3084.
- [23] C. O. Hwang, M. Mascagni and J. A. Given, A Feynman-Kac path-integral implementation for Poisson’s equation using an h-conditioned Green’s function, *Math. Comput. Simul.*, 62(3-6) (2003), pp. 347–355.
- [24] P. Kloeden, E. Platen, *Numerical Solution of Stochastic Differential Equations*, Springer, New York, 1992.
- [25] M. Kwaśnicki, Ten equivalent definitions of the fractional Laplace operator, *Fract. Calc. Appl. Anal.*, 20(1) (2017), pp. 7–51.
- [26] A. E. Kyprianou, A. Osójnik and T. Shardlow, Unbiased “walk-on-spheres” Monte Carlo methods for the fractional Laplacian, *IMA J. Numer. Anal.*, 38 (2018), pp. 1550–1578.
- [27] H. A. Lay, Z. Colgin, V. Reshniak, Abdul Q. M. Khaliq, On the implementation of multilevel Monte Carlo simulation of the stochastic volatility and interest rate model using multi-GPU clusters, *Monte Carlo Meth. Appl.*, 24(4) (2018), pp. 309–321.
- [28] C. P. Li and M. Cai, *Theory and Numerical Approximations of Fractional Integrals and Derivatives*, SIAM, Philadelphia, 2019.
- [29] C. P. Li and Z. Q. Li, Asymptotic behaviors of solution to Caputo-Hadamard fractional partial differential equation with fractional Laplacian, *Int. J. Comput. Math.*, 2020, DOI:10.1080/00207160.2020.174454.
- [30] C. P. Li and Q. Yi, Modeling and Computing of Fractional Convection Equation, *Commun. on Appl. Math. and Comput.*, 1 (2019), pp. 565–595.
- [31] A. Lischke, G. F. Pang, M. Gulian, F. Y. Song, C. Glusa, X. N. Zheng, Z. P. Mao, W. Cai, M. M. Meerschaert, M. Ainsworth, and G. E. Karniadakis, What is the fractional Laplacian? A comparative review with new results, *J. Comput. Phys.*, 404 (2020), 109009.
- [32] M. Luca and L. David, Extremely efficient acceptance-rejection method for simulating uncorrelated Nakagami fading channels, *Commun. Statistics-Simulat.Comput.*, 48(6) (2019), pp. 1798–1814.
- [33] M. E. Muller, Some continuous Monte Carlo Methods for the Dirichlet problem, *Ann. Math. Stat.*, 27(3) (1956), pp. 569–589.
- [34] K. B. Oldham and J. Spanier, *The Fractional Calculus: Theory and Applications of Differentiation and Integration to Arbitrary Order*, Academic Press, New York, London, 1974.
- [35] C. Pozrikidis, *The Fractional Laplacian*, CRC Press, Boca Raton, 2016.
- [36] X. Ros-Oton and J. Serra, The Dirichlet problem for the fractional Laplacian: regularity up to the boundary, *J. Math. Pures Appl.*, 101(3) (2014), pp. 275–302.
- [37] K. K. Sabelfeld, *Monte Carlo Methods in Boundary Value Problems*, Springer, Berlin, 1991.
- [38] Z. Zhang, Error estimate of spectral Galerkin methods for a linear fractional reaction-diffusion equation, *J. Sci. Comput.*, 78(2) (2019), pp. 1087–1110.

- Author Dashboard**
- 1 Submitted Manuscripts >
- 1 Manuscripts with Decisions >
- Start New Submission >
- Legacy Instructions >
- 5 Most Recent E-mails >
- Before You Submit >

## Manuscripts with Decisions

ACTION	STATUS	ID	TITLE	SUBMITTED	DECISIONED
a revision has been submitted (NMPDE-2020-3405.R1)	EIC: Webster, Clayton ADM: Editorial, Office	NMPDE-2020-3405	A Modified Walk-on-sphere Method for High Dimensional <a href="#">View Submission</a>	28-Jul-2020	22-Dec-2020
	<ul style="list-style-type: none"> <li>• Major Revision (22-Dec-2020)</li> <li>• a revision has been submitted</li> </ul>				
	<a href="#">view decision letter</a> <a href="#">Contact Journal</a>				